THE JOURNAL OF BIOLOGICAL CHEMISTRY VOL. 291, NO. 13, pp. 6813–6830, March 25, 2016

RipAY, a Plant Pathogen Effector Protein, Exhibits Robust γ-Glutamyl Cyclotransferase Activity When Stimulated by Eukaryotic Thioredoxins*

Received for publication, July 14, 2015, and in revised form, January 26, 2016 Published, JBC Papers in Press, January 28, 2016, DOI 10.1074/jbc.M115.678953

Shoko Fujiwara[‡], Tomoki Kawazoe[‡], Kouhei Ohnishi[§], Takao Kitagawa[¶], Crina Popa[‖], Marc Valls[‖], Stéphane Genin[**], Kazuyuki Nakamura[‡‡], Yasuhiro Kuramitsu[¶], Naotaka Tanaka[‡], and Mitsuaki Tabuchi[‡1]

*From the [‡]Department of Applied Biological Science, Faculty of Agriculture, Kagawa University, Miki-cho, Kagawa, 761-0795, Japan, the [§]Research Institute of Molecular Genetics, Kochi University, Nankoku 783-0093, Japan, the [¶]Department of Biochemistry and Functional Proteomics, Yamaguchi University Graduate School of Medicine, Ube, Yamaguchi 755-8505, Japan, the [‖]Departament de Genètica, Universitat de Barcelona and Centre for Research in Agricultural Genomics, Bellaterra, Catalonia, Spain, **INRA-CNRS, Laboratoire des Interactions Plantes-Microorganismes, UMR441-2594, Castanet-Tolosan, France, and the [‡‡]Center of Clinical Laboratories, Tokuyama Medical Association Hospital, Shunan 745-0846, Japan*

The plant pathogenic bacterium *Ralstonia solanacearum* injects more than 70 effector proteins (virulence factors) into the host plant cells via the needle-like structure of a type III secretion system. The type III secretion system effector proteins manipulate host regulatory networks to suppress defense responses with diverse molecular activities. Uncovering the molecular function of these effectors is essential for a mechanistic understanding of *R. solanacearum* pathogenicity. However, few of the effectors from *R. solanacearum* have been functionally characterized, and their plant targets remain largely unknown. Here, we show that the ChaC domain-containing effector RipAY/RSp1022 from *R. solanacearum* exhibits γ-glutamyl cyclotransferase (GGCT) activity to degrade the major intracellular redox buffer, glutathione. Heterologous expression of RipAY, but not other ChaC family proteins conserved in various organisms, caused growth inhibition of yeast *Saccharomyces cerevisiae*, and the intracellular glutathione level was decreased to ~30% of the normal level following expression of RipAY in yeast. Although active site mutants of GGCT activity were non-toxic, the addition of glutathione did not reverse the toxicity, suggesting that the toxicity might be a consequence of activity against other γ-glutamyl compounds. Intriguingly, RipAY protein purified from a bacterial expression system did not exhibit any GGCT activity, whereas it exhibited robust GGCT activity upon its interaction with eukaryotic thioredoxins, which are important for intracellular redox homeostasis during bacterial infection in plants. Our results suggest that RipAY has evolved to sense the host intracellular redox environment, which triggers its enzymatic activity to create a favorable environment for *R. solanacearum* infection.

Numerous bacterial pathogens of plants and animals inject virulence proteins, so-called effectors, directly into the host cell cytoplasm through specialized secretion apparatuses, such as the type III secretion system (T3SS).[2] The translocated T3SS effector proteins manipulate diverse host cellular processes, including cytoskeletal reorganization, signal transduction, gene expression, vesicular trafficking, autophagy, and DNA replication, to promote infection and ultimately cause disease (1, 2). Although the identification of the biochemical activities of these effector proteins is essential to understand the molecular mechanism of pathogenesis, it has been very difficult to predict the molecular functions based on their primary sequences because many effector proteins have limited similarity to known proteins and some effectors can be considered "convergently evolved" mimics of their eukaryotic cell counterparts (3). Furthermore, thanks to extensive genome sequencing programs, coupled with robust computational predictions of sequence motifs characteristic of effector proteins, the number of putative effectors identified in the genomes from many bacterial pathogens is continuously increasing in the database (4). For the above reasons, a function-based method to efficiently analyze effector proteins is desired. Interestingly, effector proteins have been observed to confer a growth inhibition phenotype when heterologously expressed in the yeast *Saccharomyces cerevisiae* (5, 6). This growth inhibition is thought to be the consequence of the effector-induced compromise of cellular processes conserved between yeast and higher eukaryotes. For example, Lesser and Miller (7) showed that the *Yersinia* effector YopE, which functions as a Rho GTPase-activating protein (RhoGAP), blocks actin polarization and cell cycle progression through its RhoGAP activity. Importantly, growth inhibition is a genetically tractable phenotype, and it provides a variety of means to investigate modes of action of these effectors toward host cell targets.

Ralstonia solanacearum, which is a widely distributed soil-borne phytopathogen, causes lethal bacterial wilt of more than 200 plant species, including economically important crops,

* This work was supported by Japan Society for the Promotion of Science KAKENHI Grants 22580095 and 25450104 and also, in part, by the General Research Grant of the Institute of Fermentation, Osaka. The authors declare that they have no conflicts of interest with the contents of this article.

[1] To whom correspondence should be addressed: Dept. of Applied Biological Science, Faculty of Agriculture, Kagawa University, 2393 Ikenobe Miki-cho, Kagawa 761-0795, Japan. Tel.: 81-87-891-3110; Fax: 81-87-891-3021; E-mail: mtabuchi@ag.kagawa-u.ac.jp.

[2] The abbreviations used are: T3SS, type III secretion system; GGCT, γ-glutamyl cyclotransferase; SD, synthetic dextrose; SGal, synthetic galactose; Tricine, *N*-[2-hydroxy-1,1-bis(hydroxymethyl)ethyl]glycine; Trx, thioredoxin.

TABLE 1
Strains used in this study

Strain	Genotype	Reference or source
S. cerevisiae		
BY4741	*MAT*a *his3Δ1 leu2Δ0 met15Δ0 ura3Δ0*	Research Genetics
BY4742	*MATα his3Δ1 leu2Δ0 lys2Δ0 ura3Δ0*	Research Genetics
BY4743	BY4741/BY4742	Research Genetics
MTY654	BY4741 *dug3Δ::KanMX4 ecm38Δ::KanMX4 gcg1Δ::KanMX4*	This study
MTY674	BY4741 *trx1Δ::KanMX4*	This study
MTY676	BY4741 *trx2Δ::KanMX4*	This study
MTY678	BY4741 *trx3Δ::KanMX4*	This study
MTY680	BY4741 *trx1Δ::KanMX4 trx2Δ::KanMX4*	This study
MTY761	BY4741 *trx1Δ::KanMX4 trx2Δ::KanMX4 trx3Δ::KanMX4*	This study
gsh1Δ/gsh1Δ	BY4743 *gsh1Δ::KanMX4/gsh1Δ::KanMX4*	Research Genetics
AH109	*MATa trp1-901 leu2-3 112 ura3-52 his3-200 gal4Δ gal80Δ LYS2::GAL1*$_{UAS}$*-GAL1*$_{TATA}$*-HIS3 MEL1 GAL2*$_{UAS}$*-GAL2*$_{TATA}$-ADE2 URA3::*MEL1*$_{UAS}$*-MEL1*$_{TATA}$*-LacZ*	Clontech
R. solanacearum		
OE1-1	Wild-type, pathogenic to tobacco, eggplant isolate	Ref. 25
RK5081	OE1-1 Δ*hrcU-1*	This study
RK7101	OE1-1 Δ*ripAY-4*	This study

such as tomato, potato, and tobacco (8). Among the pathogenicity determinants of this bacterium, T3SS was shown to play an essential role in pathogenicity because the corresponding mutants were avirulent on host plants (9). In general, compared with animal pathogens, bacterial plant pathogens, such as *Xanthomonas* spp. or *Pseudomonas syringae*, contain larger numbers (~30–40) of effectors, but the *R. solanacearum* effector repertoire is exceptionally large, probably due to its wide host range (10). Postgenomic functional analyses using regulation-based approaches and/or T3SS-translocon assays have identified the nearly complete repertoire of 70–75 effectors in the reference strain GMI1000 and the phylogenetically close strain RS1000 (11). The investigation of the *R. solanacearum* strain complex pangenome also identified additional families of likely effector proteins with no homology to other previously identified effectors, and thus the current estimated number of effector families is ~110 among 11 strains representative of the biodiversity of the *R. solanacearum* strain complex (12). Individual *R. solanacearum* strains typically possess around 60–75 effectors. Effector repertoire comparison revealed a group of 32 core effectors present in 10 of 11 strains (13). To date, only a few *R. solanacearum* effectors have been assigned molecular functions and targets (14–16), but most of these effectors remain functionally uncharacterized.

In this study, we screened *R. solanacearum* effectors using a yeast expression system and identified RipAY as an effector whose expression causes growth inhibition in yeast. RipAY, which is one of the *R. solanacearum* core effectors, has previously been shown experimentally to be an effector injected into host plant cells via T3SS (17), but the molecular function of this effector has yet to be characterized. Bioinformatics analysis revealed that RipAY contains a ChaC domain, which is a conserved domain found in all phyla examined but whose molecular function was totally unknown when we started our study. Recently, it has been reported that yeast and mammalian ChaC domain-containing proteins exhibit γ-glutamyl cyclotransferase (GGCT) activity specifically to degrade glutathione (18). We demonstrated that RipAY exhibits robust GGCT activity and significantly decreases intracellular glutathione in yeast. Surprisingly, we failed to detect GGCT activity of recombinant RipAY expressed in *Escherichia coli*. However, we could detect robust GGCT activity when RipAY was activated by yeast or plant thioredoxins. Both glutathione and thioredoxins are important for maintaining cellular redox homeostasis and also indispensable for proper activation of plant innate immunity during pathogen infection (19, 20). Together, our data provide new evidence that *R. solanacearum* perturbs the host redox environment to allow bacterial infection.

Experimental Procedures

Strains, Plasmids, and Media—Descriptions of the strains and plasmids used in this study are presented in Tables 1–3. *Escherichia coli* DB3.1 (Life Technologies, Inc.) was used for the construction and amplification of the Gateway™ vectors, and *E. coli* DH5α or JM109 was the bacterial host for all of the other plasmids constructed. Coding sequences were amplified by PCR using KOD-Plus-Neo polymerase (Toyobo) or PrimeSTAR GXL polymerase (Takara Bio). Plasmids were sequenced to ensure that no mutations were introduced due to manipulations. Yeast transformation was performed using the lithium acetate method (21). Mutant constructs were generated by site-directed mutagenesis (22) and confirmed by sequencing. The media used for yeast culture were synthetic dextrose (SD) medium (2% glucose, 0.67% yeast nitrogen base without amino acids) and synthetic galactose (SGal) medium (2% galactose, 0.67% yeast nitrogen base without amino acids). Appropriate amino acids and bases were added to SD or SGal medium as necessary. Yeast cells were cultured at 26 °C unless otherwise stated.

Phylogenetic Analysis—Phylogenetic trees of ChaC domain-containing proteins, including RipAY or thioredoxins from various organisms, were created with MEGA6 (23). The amino acid sequences of ChaC proteins or thioredoxins from the NCBI database were aligned with ClustalW, from which a maximum likelihood phylogenetic tree was created.

Homology Modeling and Structure Analysis—The RipAY protein sequence was used for fold recognition using the Phyre2 server. This search identified human GGCT (C7 orf24, Protein Data Bank entries 2PN7 and 2RBH) as the best template. We used the alignment provided by the Phyre2 server to construct models for RipAY using CueMol molecular graphics software.

TABLE 2
***S. cerevisiae* plasmids used in this study**

Plasmids	Construct	Reference or source
pMT751	*URA3, 2μ, P_{GAL1}-att*R1-*Cm^r-ccd*B-*att*R2-GFP	Ref. 33
pMT830	*URA3, 2μ, $P_{tet\text{-}off}$-att*R1-*Cm^r-ccd*B-*att*R2-GFP	Ref. 33
pMT1373	*URA3, 2μ, P_{GAL1}-att*R1-*Cm^r-ccd*B-*att*R2-Protein A	This study
pGBKT7	*TRP1, 2μ*, yeast two-hybrid *GAL4* DNA-BD vector	Clontech
pGADT7	*LEU2, 2μ*, yeast two-hybrid *GAL4* AD vector	Clontech
pACT2	*LEU2, 2μ*, yeast two-hybrid *GAL4* AD vector	Clontech
pMT731	pACT2; *GAL4* AD-*att*R1-*Cm^r-ccd*B-*att*R2	This study
pMT922	pMT830; *URA3, 2μ, $P_{tet\text{-}off}$*-GFP	Ref. 33
pRE85	pMT751; *URA3, 2μ, P_{GAL1}-R. sonalacearum RipAY*-GFP	This study
pRE97	pMT751; *URA3, 2μ, P_{GAL1}-R. sonalacearum RSc0782*-GFP	This study
pRE98	pMT751; *URA3, 2μ, P_{GAL1}-H. sapiens Chac2*-GFP	This study
pRE99	pMT751; *URA3, 2μ, P_{GAL1}-P. syringae PSPTO_5239*-GFP	This study
pRE100	pMT751; *URA3, 2μ, P_{GAL1}-S. cerevisiae GCG1*-GFP	This study
pRE161	pMT751; *URA3, 2μ, P_{GAL1}-A. citrulli Aave_4606*-GFP	This study
pRE173	pMT751; *URA3, 2μ, P_{GAL1}-A. thaliana AT1G44790/GGCT2;3*-GFP	This study
pRE174	pMT751; *URA3, 2μ, P_{GAL1}-A. thaliana AT4G31290/GGCT2;2*-GFP	This study
pRE175	pMT751; *URA3, 2μ, P_{GAL1}-A. thaliana AT5G26220/GGCT2;1*-GFP	This study
pRE86	pMT751; *URA3, 2μ, P_{GAL1}-RipAY^{E216Q}*-GFP	This study
pRE164	pMT751; *URA3, 2μ, P_{GAL1}-RipAY2^{Y129A}*-GFP	This study
pRE165	pMT751; *URA3, 2μ, P_{GAL1}-RipAY^{L130A}*-GFP	This study
pRE166	pMT751; *URA3, 2μ, P_{GAL1}-RipAY^{S131A}*-GFP	This study
pRE167	pMT751; *URA3, 2μ, P_{GAL1}-RipAY^{L132A}*-GFP	This study
pRE168	pMT751; *URA3, 2μ, P_{GAL1}-RipAY^{L130G}*-GFP	This study
pSF38	pMT751; *URA3, 2μ, P_{GAL1}-RipAY^{C333S}*-GFP	This study
pRE257	pMT1373; *URA3, 2μ, P_{GAL1}-S. cerevisiae GCG1*-Protein A	This study
pRE258	pMT1373; *URA3, 2μ, P_{GAL1}-RipAY*-Protein A	This study
pRE259	pMT1373; *URA3, 2μ, P_{GAL1}-RipAY^{E216Q}*-Protein A	This study
pSF25	pGBKT7; *TRP1, 2μ, P_{ADH1}-GAL4 DNA-BD-RipAY^{E216Q}*	This study
pSF37	pGBKT7; *TRP1, 2μ, P_{ADH1}-GAL4 DNA-BD-RipAY^{E216Q,C333S}*	This study
pRE249	pGADT7; *LEU2, 2μ, P_{ADH1}-GAL4 AD-A. thaliana TRX h2*	This study
pRE250	pGADT7; *LEU2, 2μ, P_{ADH1}-GAL4 AD-A. thaliana TRX h3*	This study
pSF50	pMT731; *LEU2, 2μ, P_{ADH1}-GAL4 AD-A. thaliana TRX h5*	This study
pSF51	pMT731; *LEU2, 2μ, P_{ADH1}-GAL4 AD-A. thaliana TRX h5^{C39S,C42S}*	This study
pSF52	pMT731; *LEU2, 2μ, P_{ADH1}-GAL4 AD-S. cerevisiae TRX1*	This study
pMT1416	pMT731; *LEU2, 2μ, P_{ADH1}-GAL4 AD-R. solanacearum TrxA*	This study
pTEF1-416-*HGT1*	pRS416; *URA3, CEN, P_{TEF1}-S. cerevisiae HGT1*	Ref. 31

TABLE 3
***E. coli* plasmids used in this study**

Plasmids	Construct	Reference or source
pET23d	*Amp, P_{T7}*, the C-terminal His_6 tag fusion vector	Novagen, Inc.
pDEST17	*Amp, P_{T7}*, the Gateway N-terminal His_6 tag fusion vector	Life Technologies, Inc.
pMT1371	pET23d: *P_{T7}-attR1-Cm^r-ccd*B-*att*R2-Protein A	This study
pSF16	pET23d: *P_{T7}-R. solanacearum RipAY*-His_6	This study
pSF17	pET23d: *P_{T7}-S. cerevisiae GCG1*-His_6	This study
pSF16	pET23d: *P_{T7}-R. solanacearum RipAY*-His_6	This study
pSF40	pET23d: *P_{T7}-S. cerevisiae TRX1*-His_6	This study
pSF49	pDEST17: *P_{T7}*-Met-His_6-*A. thaliana TRX h5*	This study
pMT1293	pET23d: *P_{T7}-S. cerevisiae DUG1*-His_6	This study
pMT1409	pDEST17: *P_{T7}*-Met-His_6-*A. thaliana TRX h2*	This study
pMT1410	pDEST17: *P_{T7}*-Met-His_6-*A. thaliana TRX h3*	This study
pMT1411	pDEST17: *P_{T7}*-Met-His_6-*A. thaliana TRX h5^{C39S,C42S}*	This study
pMT1415	pDEST17: *P_{T7}*-Met-His_6-*R. solanacearum TrxA*	This study
pMT1368	pMT1371: *P_{T7}*-Protein A	This study
pRE254	pMT1371: *P_{T7}-S. crevisiae GCG1*-Protein A	This study
pRE255	pMT1371: *P_{T7}-R. solanacearum RipAY*-Protein A	This study
pRE256	pMT1371: *P_{T7}-R. solanacearum RipAY^{E216Q}*-Protein A	This study
pRE496	pMT1371: *P_{T7}-R. solanacearum RipAY^{C333S}*-Protein A	This study

Production and Purification of Recombinant Proteins in E. coli—For the purification of the His_6-tagged recombinant proteins, Rosetta-gami B (DE3) cells (EMD) carrying pMT1293, pMT1409, pMT1410, pMT1411, pMT1415, pSF16, pSF17, pSF40, or pSF49 plasmid were grown in 600 ml of Luria-Bertani (LB) medium with 34 μg/ml chloramphenicol and 100 μg/ml ampicillin at 37 °C to an A_{600} of 0.8. The bacteria were then moved to 18 °C for 30 min, and the protein expression was induced by the addition of isopropyl-1-thio-β-D-galactopyranoside to 0.3 mM for 6 h. The cells were collected by centrifugation at 10,000 × *g* for 5 min. The cell pellet was resuspended in 30 ml of binding buffer (50 mM NaH_2PO_4, 500 mM NaCl, 5 mM imidazole, pH 8.0) containing 1 mM PMSF and disrupted by sonication. The lysate was cleared by centrifugation at 10,000 × *g* for 30 min at 4 °C, and the cleared lysate was applied to the HisTrap FF 1-ml column (GE Healthcare) equilibrated with binding buffer. The column was then washed with a 20-column volume of binding buffer and eluted with elution buffer (50 mM NaH_2PO_4, 500 mM NaCl, 300 mM imidazole, pH 8.0). Fractions containing the recombinant His_6-tagged fusion proteins were collected. Purified His_6-tagged thioredoxins were treated with 20 mM dithiothreitol (DTT) at room temperature for 15 min to reduce thioredoxins. Purified proteins were subsequently dialyzed into PBS, and protein concentra-

tions were determined using a micro-BCA protein assay kit (Thermo Scientific).

Measurement of Cys-Gly Peptidase (Dug1)-coupled GGCT Activity of His_6-tagged RipAY and Gcg1 Purified from E. coli—GGCT activity toward glutathione as substrate was carried out using a Dug1-coupled assay as described previously (18) with some modifications. In brief, 0.4 μM Gcg1 or 0.04 μM RipAY with appropriate concentrations of the cell lysates from various organisms or thioredoxins purified from *E. coli* was incubated with glutathione for 20 min at 37 °C in 50 μl of reaction mixture containing 50 mM Tris-HCl (pH 8.0). The reaction was terminated by the addition of 20 μl of 0.25 N HCl and then neutralized with the addition of 8.4 μl of 1 M Tris and made up to 100 μl with 50 mM Tris-HCl (pH 8.0). Ten microliters of the reaction mixture was then transferred to a new tube to which was added 2 μl of Dug1 reaction mixture; this converts the Cys-Gly dipeptide into free cysteine and glycine. The Dug1 reaction mixture consisted of 20 μM $MnCl_2$ and 1 μg of recombinant *S. cerevisiae* Dug1p, a Cys-Gly peptidase purified from *E. coli*. This reaction mixture was further incubated for 1 h at 37 °C. The free cysteine generated was measured by acidic ninhydrin solution (20 g of ninhydrin dissolved in acetic acid and HCl that are mixed in a 3:2 ratio) and added to the reaction mixture, and the reaction mixture was incubated at 100 °C for 10 min to develop the pink color. Two hundred microliters of colored solutions was transferred to a 96-well plate, and the A_{570} was measured using a microplate reader (Bio-Rad). The assay was performed in triplicates, and data are mean ± S.E.

Measurement of GGCT Activity of Protein A-tagged RipAY and Gcg1—*GCG1*, *ripAY*^{WT}, or *ripAY*^{E216Q} genes on pDONR221 donor vector were cloned into the Protein A-tagging gateway destination vectors, pMT1371 for *E. coli* or pMT1373 for *S. cerevisiae*, by the LR reaction. *E. coli* Rosetta gami B (DE3) cells carrying pMT1371-*GCG1*, *ripAY*^{WT}, *ripAY*^{E216Q}, or *ripAY*^{C333S} plasmids were cultured in 100 ml of LB medium containing 34 μg/ml chloramphenicol and 100 μg/ml ampicillin at 37 °C to an A_{600} of 0.8. The bacteria were then moved to 18 °C for 30 min, and the protein expression was induced by the addition of isopropyl-1-thio-β-D-galactopyranoside to 0.3 mM for 6 h. *E. coli* cells expressing Protein A-tagged Gcg1, RipAY^{WT}, RipAY^{E216Q}, or RipAY^{C333S} proteins were suspended in IPP150 buffer (10 mM Tris-HCl, pH 8.0, 150 mM NaCl, 50 mM EDTA) and disrupted by sonication to generate the *E. coli* lysates. *S. cerevisiae* cells carrying pMT1373-*GCG1*, *ripAY*^{WT}, or *ripAY*^{E216Q} plasmids were cultured in 20 ml of SD (−Ura) liquid medium at 26 °C to an A_{600} of 1.0, and then cells were washed twice with sterilized water and resuspended in 20 ml of SGal (−Ura) liquid medium and cultured at 26 °C for 17 h to induce the protein expressions. *S. cerevisiae* cells expressing Protein A-tagged Gcg1, RipAY^{WT}, or RipAY^{E216Q} proteins were suspended in 500 μl of 1 M sorbitol, 50 mM EDTA solution containing 10 mM DTT with 1 mg of Zymolyase-20T (Nakarai Tesque Inc.) to obtain spheroplasts. Spheroplasts were washed once with 1 M sorbitol, 50 mM EDTA and resuspended with 1 ml of IPP150 buffer containing 2 μM pepstatin A and 1 mM PMSF and homogenized with a Dounce homogenizer (10 strokes) on ice to generate the *S. cerevisiae* lysates. The lysates from *E. coli* or *S. cerevisiae* cells were cleared by centrifugation at 10,000 × *g* for 30 min at 4 °C, and 50 μl of IgG-Sepharose beads (50%, v/v) were added into the cleared lysate and incubated for 2 h at 4 °C on a rotating wheel. The beads were washed three times with the same buffer. The Protein A-tagged fusion protein-immobilized beads were used for measuring the GGCT activity by a Dug1-coupled method as described above. For activation of affinity-purified Protein A-tagged RipAY from *E. coli*, the Protein A-tagged fusion protein-immobilized beads were incubated with the total protein lysate from yeast cells in 1 ml of IPP150 buffer at 4 °C for 2 h, washed three times with IPP150 buffer, and then used for measuring the GGCT activity by a Dug1-coupled method as described above.

Immunoblotting Analysis—Yeast cells expressing GFP-tagged RipAY or other ChaC proteins were collected and resuspended in 1 ml of PBS. After the addition of trichloroacetic acid (TCA) to a final concentration of 10%, cells were incubated on ice for 15 min and precipitated by centrifugation. TCA-treated yeast cells were washed twice with 1 ml of ice-cold acetone and dried. Total proteins were extracted from the dried cells by beating cells with glass beads (two pulses of 5 min each at 65 °C) in Urea-SDS cracking buffer (6 M urea, 1% SDS, 50 mM Tris-HCl, pH 7.5). The total protein concentration of the cell extracts was determined using a micro-BCA protein assay kit (Thermo Scientific). Ten-microgram aliquots of total protein were subjected to immunoblotting analysis, which was performed using affinity-purified rabbit anti-GFP antiserum (our laboratory stock) or rabbit anti-glucose-6-phosphate dehydrogenase antibody (Sigma, A9521) and horseradish peroxidase-conjugated anti-rabbit IgG serum (Cell Signaling Technologies). Signals were detected using Immunostar LD Western blotting detection reagent (Wako).

Measurement of Total Cellular Glutathione—Ten A_{600} of yeast cells expressing RipAY and their mutants under the control of the *GAL1* promoter were washed once with 1 ml of KPE (0.1 M potassium phosphate buffer with 5 mM EDTA, pH 7.5) and lysed in 200 μl of 5% sulfosalicylic acid using glass beads. Cells were vortexed for 1 min with 1-min intervals 10 times and centrifuged for 10 min at 4 °C. Total cellular glutathione in yeast was measured as described previously (24). In brief, 10 μl of supernatant was mixed with 60 μl of DTNB (2 mg/3 ml) and 60 μl of glutathione reductase (2.5 units/ml) in a 96-well plate. Sixty microliters of NADPH (2 mg/3 ml) was added in the above mixtures to start the reaction. Absorbance was measured at every 15 s at 415 nm. Absorbance at 2 min was used to compare the glutathione level in the different samples. Total cellular glutathione in yeast is normalized to A_{600} of yeast cells.

Measurement of Total Cellular Glutathione in Bacteria-inoculated Plants—A 10^8-cfu/ml suspension of *R. solanacearum* OE1-1 (WT) (25), RK5081 (T3SS mutant, Δ*hrcU-1*), or RK7101 (Δ*ripAY-4*) in a ~50 μl volume was inoculated into fully expanded leaves of 6–8-week-old susceptible eggplant (*Solanum melongena* cv. Senryo 2-gou) using a needleless disposable syringe, and the bacteria-inoculated plants were maintained in a greenhouse facility. Two leaf disks (0.8 cm^2 each) were taken 1 day after inoculation and frozen in liquid nitrogen. The frozen samples were extracted by shaking five times with 5-mm diameter stainless beads for 30 s in a 2.0-ml screw-capped vial using

a bead beater device. Three hundred microliters of 5% sulfosalicylic acid in KPE was added to the samples, and then the samples were vortexed and centrifuged at 8,000 × *g* for 20 min at 4 °C. Total cellular glutathione of the samples extracted from bacteria-inoculated plants was measured by the same method as used for the samples from yeast as described above. Total cellular glutathione in bacteria-inoculated leaf was normalized to mg of leaf material.

Fluorescent Microscopic Analysis—Fluorescence of GFP in the non-fixed yeast cells was observed using an Olympus BX51 microscope (Olympus) with a GFP filter. Images were captured with a Hamamatsu C11440-10C Orca-Flash 2.8 CMOS camera (Hamamatsu Photonics) using Metamorph software (Molecular Devices).

Yeast Two-hybrid Analysis—The yeast two-hybrid analysis was performed using a *GAL4*-based yeast two-hybrid system according to the manufacturer's instructions (MATCHMAKER Two-Hybrid System 3; Clontech). RipAY with the E216Q active site mutation ($RipAY^{E216Q}$) was used for yeast two-hybrid analysis to avoid the growth inhibition caused by its expression in yeast. The $ripAY^{E216Q}$ gene was amplified by PCR and cloned into the EcoRI and BamHI sites of pGBKT7 vector to generate a construct of $RipAY^{E216Q}$ fused in-frame to the Gal4 DNA-binding domain as the bait. Gateway™ technology (Life Technologies) was used to construct the prey plasmids. Thioredoxin cDNAs (*R. solanacearum* TrxA/RSc1188, *S. cerevisiae* Trx1, and *Arabidopsis thaliana* Trx-h2, Trx-h3, and Trx-h5) were amplified by PCR and cloned into the gateway donor vector pDONR221 by the BP reaction. The pDONR221-Trx-h5 plasmid was used to introduce the C39S,C42S active site mutation into Trx-h5. The thioredoxin genes on pDONR221 plasmid were cloned into pACT2-based gateway Gal4 activation domain plasmid, pMT731, by the LR reaction to generate the prey plasmids. The bait and prey plasmids were cotransformed into two-hybrid reporter yeast strain AH109 cells. The transformants were spotted on SD (−Trp, −Leu) plates and SD plates with different stringency conditions (low: −Trp, −Leu, −His; medium: −Trp, −Leu, −His, + 1 mM 3-amino-1,2,4-triazole; high: −Trp, −Leu, −His, −Ade), and the interaction of RipAY and thioredoxins was assessed by their growth under the different stringency conditions.

Purification of the RipAY Activator from Yeast—Soluble proteins were extracted from 10 g of *S. cerevisiae* MTY654 (*dug3*Δ *ecm38*Δ *gcg1*Δ) cells mechanically disrupted by a French press. The extracted *S. cerevisiae* proteins were precipitated with 100% ammonium sulfate. Precipitated proteins were dialyzed overnight at 4 °C against 6 liters of 20 mM Tris-HCl, pH 7.5. *S. cerevisiae* proteins were separated over a HiPrep DEAE FF 16/10 ion exchange column with a salt gradient from 0 to 1 M NaCl (GE Healthcare). Individual fractions were assayed for their ability to stimulate GGCT activity of a recombinant RipAY purified from *E. coli*. Fractions possessing the majority of activity were pooled and dialyzed overnight at 4 °C against 2 liters of 20 mM Tris-HCl, pH 7.5, 1.5 M $(NH_4)_2SO_4$. After dialysis, *S. cerevisiae* proteins were separated on a HiPrep Butyl FF 16/10 hydrophobic interaction column with a salt gradient from 1.5 to 0 M $(NH_4)_2SO_4$ (GE Healthcare). Individual fractions retaining the activity were pooled and concentrated to 1 ml using an Amicon Ultra-2mL 3K centrifugal filter device (Millipore). Positive fractions were then separated over a HiPrep 16/60 Sephacryl 200 high resolution gel filtration column (GE Healthcare). Proteins in this final purification step contained in the positive fraction were separated by Tricine SDS-PAGE and visualized with a Sil-Best Stain One (Nakarai Tesque Inc.) or a Coomassie Brilliant Blue stain.

In-gel digestion and the following LC-MS/MS analysis of the activator protein from yeast were performed as described previously (26). Protein identification was performed in the Agilent Spectrum MILL MS proteomics workbench against the Swiss-Prot protein database search engine.

Statistical Analysis—Statistical analysis was performed using GraphPad Prism version 6 or Microsoft Excel software and specific tests noted throughout.

Results

Expression of a ChaC Domain-containing Effector, RipAY, Causes Growth Inhibition of Yeast—To understand the molecular mechanism of pathogenesis for *R. solanacearum*, we screened the collection of 36 previously identified effector proteins of *R. solanacearum* GMI1000 (13, 27) using a yeast galactose-inducible expression system. This yeast expression screen revealed eight effectors that cause growth inhibition of yeast *S. cerevisiae*. Details of this screen along with the complete set of identified effectors will be described elsewhere.[3]

To predict the molecular function of the identified effectors, we first searched for the functional domain or motif using the Pfam search engine based on their primary sequences. One of the identified effectors, RipAY (locus tag RSp1022) contains a ChaC domain, originally identified in a protein encoded by *E. coli chaC* and assumed to be a possible regulator of the *cha* operon (Ca^{2+}/H^+ antiporter) (28). Orthologues of the ChaC protein are found in all phyla examined. We investigated the phylogenic relationship of the protein with other ChaC protein sequences from various organisms. RipAY and Aave_4606 identified in the genome of the cucurbit pathogenic bacterium *Acidovorax citrulli* (referred to as the class II ChaC protein family) are clearly an out-group of the ChaC proteins conserved in various organisms (referred to as the class I ChaC protein family) in a phylogenic reconstruction (Fig. 1*A*). Interestingly, both the *R. solanacearum* and *A. citrulli* genome contain another ChaC protein (RSc0782 and Aave_2801, respectively), which belongs to the class I ChaC protein family. RipAY and Aave_4606 have N- and C-terminal extension sequences outside of their ChaC domains and are much larger than the class I ChaC proteins (~400 amino acids for class II *versus* ~200 amino acids for class I) (Fig. 1*B*). The ChaC domain of RipAY shows lower identity to that of the class I ChaC proteins (6.2–21.3%) but higher identity to that of the class II ChaC protein, Aave_4606 (46.4%) (Fig. 1*B*). It seems that RipAY and Aave_4606 most probably originated from a duplication of the class I ChaC protein family genes and evolved to acquire a specific function as an effector.

[3] J. Hasegawa, T. Nakagawa, S. Fujiwara, N. Tanaka, and M. Tabuchi, manuscript in preparation.

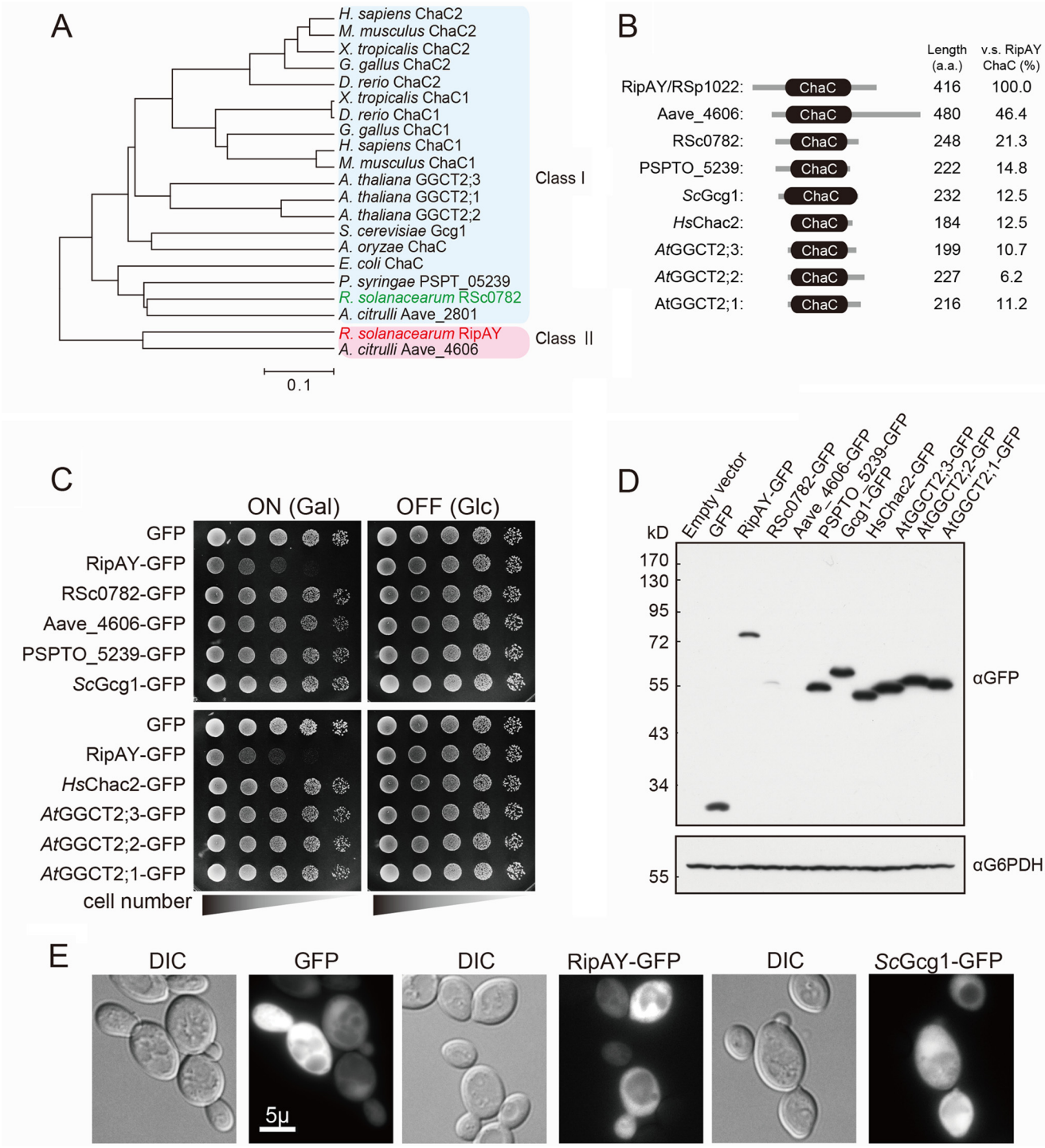

FIGURE 1. **Expression of RipAY, but not other ChaC family proteins from various organisms, causes growth inhibition of yeast.** *A*, phylogenetic analysis of ChaC domain containing proteins from various organisms. The organisms, locus tag/gene name, and Genbank™ accession numbers (in parentheses) are as follows: *E. coli* ChaC (L28709.1); *R. solanacearum* RSc0782 (AL646052.1) and RSp1022/RipAY (AL646053.1); *A. citrulli* Aave_2801 (CP000512.1) and Aave_4606 (CP000512.1); *P. syringae* PSPT_05239 (AE016853.1); *S. cerevisiae* YER163c/Gcg1 (NM_001179053.3); *Aspergillus oryzae* ChaC (XM_001818295.2); *Homo sapiens* ChaC1 (NM_001142776.1) and ChaC2 (NM_001008708.2); *Mus musculus* ChaC1 (NM_026929.4) and ChaC2 (NM_026527.3); *Xenopus tropicalis* ChaC1 (NM_001130284.1) and ChaC2 (NM_001017137.2); *Gallus gallus* ChaC1 (NM_001199656.1) and ChaC2 (AJ720918.1); *Danio rerio* ChaC1 (NM_001110126.1) and ChaC2 (BC154137.1); *A. thaliana* AT5G26220/GGCT2;1 (BT005234.1), AT4G31290/GGCT2;2 (BT006411.1), and AT1G44790/GGCT2;3 (BT006192.1). *B*, schematic representation of putative domain organization of ChaC domain-containing proteins from various organisms. *C*, yeast growth inhibition assay showing serial dilutions of *S. cerevisiae* BY4743 cells grown under inducing (galactose) or noninducing (glucose) conditions that are carrying plasmids expressing the indicated C-terminal GFP-tagged proteins under the control of the *GAL1* promoter. The cells were grown at 26 °C for 2 days for SD (−Ura) and 3 days for SGal (−Ura). *D* and *E*, detections of the ChaC domain-containing proteins expressed in yeast. Yeast cells carrying the plasmids expressing GFP-tagged RipAY or other ChaC proteins under the control of the *GAL1* promoter were grown in SD (−Ura) liquid medium to mid-log phase and then shifted to SGal (−Ura) liquid medium to induce the protein expression, further cultured for 12 h, and analyzed by immunoblotting with anti-GFP antibody (*D*) or fluorescence microscopy with native GFP fluorescence (*E*). Glucose 6-phosphate dehydrogenase (*G6PDH*) was used as a loading control. *Scale bar*, 5 μm. *DIC*, differential interference contrast.

We next examined whether heterologous expression of the other ChaC proteins also caused growth inhibition of yeast as observed in that of RipAY (Fig. 1*C*). Expression of neither GFP alone nor the GFP-tagged C terminus of other ChaC proteins showed any impact on yeast growth (Fig. 1*C*); nonetheless, the protein expression level, except for RSc0782 and Aave_4606, was even higher than that of RipAY in yeast (Fig. 1*D*). We failed to detect the expression of the Aave_4606-GFP fusion protein in yeast, probably because the Aave_4606 gene has a high GC content (73%) and many rare codons for yeast (34 rare codons (CGC or CGG) of 38 total codons for arginine) (data not shown). We also examined the localization of the proteins in yeast cells using the native fluorescence of GFP fused at their C termini and found GFP fluorescence of RipAY and most of the other ChaC proteins expressed in the cytoplasm of yeast cells (Fig. 1*E*).[4] These results suggest that RipAY affects the cytoplasmic component(s) with different activities from the other ChaC proteins.

Expression of RipAY in Yeast Causes a Decrease in Intracellular Glutathione via Its GGCT Activity—Recently, it has been reported that the class I ChaC proteins from yeast, plants, and mammals function as GGCTs acting specifically to degrade glutathione but not other γ-glutamyl peptides (Fig. 2*A*) (18, 29). The ChaC domain of RipAY has limited similarity to that of the class I ChaC proteins (Fig. 1*B*). However, the structure of RipAY modeled on the Phyre2 website indicated that it closely resembles the structure of human GGCT (C7orf24) (30) (Fig. 2, *B* and *C*). There is a very high structural similarity between RipAY and GGCT, although there is little amino acid similarity (data not shown). The Phyre2 search showed that most key residues in the catalytic domain of GGCT aligned with corresponding residues of RipAY (Fig. 2*C*). Furthermore, multiple sequence alignment of the ChaC proteins from various organisms revealed that RipAY contains the signature motifs for the substrate binding site (Y^{129}*X*SL) and catalytic glutamate residue (Glu^{216}) (Fig. 2*D*), indicating that it may function in a similar manner.

To ask directly whether RipAY had GGCT activity toward glutathione, we first determined the GGCT activity of RipAY expressed in yeast. In this regard, we employed a Protein A tag to affinity-purify the proteins using IgG-beads directly from the Protein A-tagged RipAY-expressing yeast lysates and then determined GGCT activity of the beads bound with RipAY protein using a Dug1-coupled assay for ChaC family proteins (18). To prevent contamination of endogenous glutathione-degrading enzymes from the yeast lysate, we used a glutathione-degrading enzyme-deficient strain (*dug3*Δ *ecm38*Δ *gcg1*Δ triple mutant) to express the Protein A-tagged ChaC proteins in yeast cells. Consistent with a previous report (18), the beads bound with yeast class I ChaC family protein Gcg1 showed significant GGCT activity (Fig. 2*E*). Remarkably, we detected robust GGCT activity in the beads bound with wild-type RipAY ($RipAY^{WT}$) but not with the catalytically inactive mutant RipAY ($RipAY^{E216Q}$). Interestingly, $RipAY^{WT}$ showed ~4.5 times higher activity than that of the beads bound with Gcg1, although the amount of the $RipAY^{WT}$ protein was much lower than that of Gcg1 (Fig. 2*F*). This result demonstrated that RipAY protein purified from yeast possesses GGCT activity toward glutathione *in vitro*.

To ask whether yeast growth inhibition was caused by the GGCT activity of RipAY, we next performed a mutational analysis of the putative catalytic residues in the ChaC domain of RipAY and then assessed the mutants using the yeast growth inhibition test (Fig. 2*G*). Substitution of the putative catalytic glutamate residue to glutamine (E216Q) or the conserved substrate-binding site to alanine (Y129A, S131A, and L132A) almost completely restored the yeast growth inhibition caused by expression of RipAY. However, the substitution of non-conserved leucine at position 130 (Leu^{130}) to alanine (L130A) resulted in only weak restoration. Furthermore, the mutation of Leu^{130} to glycine, L130G, which mimics the substrate-binding site of the class I ChaC protein, could partially restore the growth, indicating that RipAY may have a different substrate binding mechanism from that of the class I ChaC proteins. Immunoblots were probed with anti-GFP (for RipAYs) and anti-glucose-6-phosphate dehydrogenase (as an internal control) antibodies, revealing similar amounts of RipAY-GFP proteins (Fig. 2*H*).

We next examined whether expression of RipAY proteins affected the intracellular glutathione level in yeast (Fig. 2*I*). Cells overexpressing Gcg1 showed a modest decrease in glutathione (decreased to 69% relative to the control). Interestingly, cells expressing $RipAY^{WT}$ led to a marked decrease in glutathione (decreased to 29% relative to the control), whereas cells expressing $RipAY^{E216Q}$ did not show a significant glutathione decrease. Together, these data showed that RipAY functions as a GGCT both *in vitro* and *in vivo*.

Addition of Exogenous Glutathione Did Not Restore RipAY-dependent Growth Inhibition in Yeast—We next investigated the effect of the addition of exogenous glutathione on the growth of RipAY-expressing yeast cells. Unexpectedly, the addition of exogenous glutathione could not restore the RipAY-dependent growth inhibition in both yeast WT and *gsh1*Δ mutant, which has a defect in endogenous glutathione synthesis (Fig. 3*A*). Interestingly, expression of the conserved substrate-binding site mutant (Y129A), whose expression does not cause growth inhibition in WT cells, causes growth inhibition in *gsh1*Δ mutant cells on medium containing 1 μM glutathione, but an excess of glutathione (100 μM) could restore this growth inhibition. Based on this result, we hypothesized that the kinetics of glutathione degradation by RipAY is much faster than that of glutathione uptake by plasma membrane glutathione transporter, Hgt1 (31). As a consequence, available glutathione is limited in yeast cells expressing RipAY, causing growth inhibition. To confirm this hypothesis, we investigated the effect of overexpression of Hgt1 in yeast cells expressing RipAY. Overexpression of Hgt1 using the strong constitutive *TEF1* promoter conferred a glutathione-sensitive phenotype to yeast WT cells (Fig. 3*B*) as reported previously (32) and showed an increased intracellular glutathione level (426 ± 39% for the 30-min culture with glutathione and 249 ± 23% for the 19-h culture with glutathione relative to that of control cells) when cells were cultured in medium containing 100 μM glutathione

[4] S. Fujiwara and M. Tabuchi, unpublished result.

(Fig. 3, *C* and *D*). Surprisingly, we observed that overexpression of Hgt1 could not restore the RipAY-dependent growth inhibition on medium containing 100 μM glutathione (Fig. 3*B*), although the intracellular glutathione level was restored (181 ± 10% for the 30-min culture with glutathione and 91 ± 15% for the 19-h culture with glutathione relative to that of control cells) in these conditions (Fig. 3, *C* and *D*). Collectively, these results indicate that RipAY has another target(s) besides glutathione, at least in yeast.

Inoculation of R. solanacearum into Eggplant Leaves Causes a Decrease in Intracellular Glutathione—To explore the function of RipAY in host plant cells during *R. solanacearum* infection,

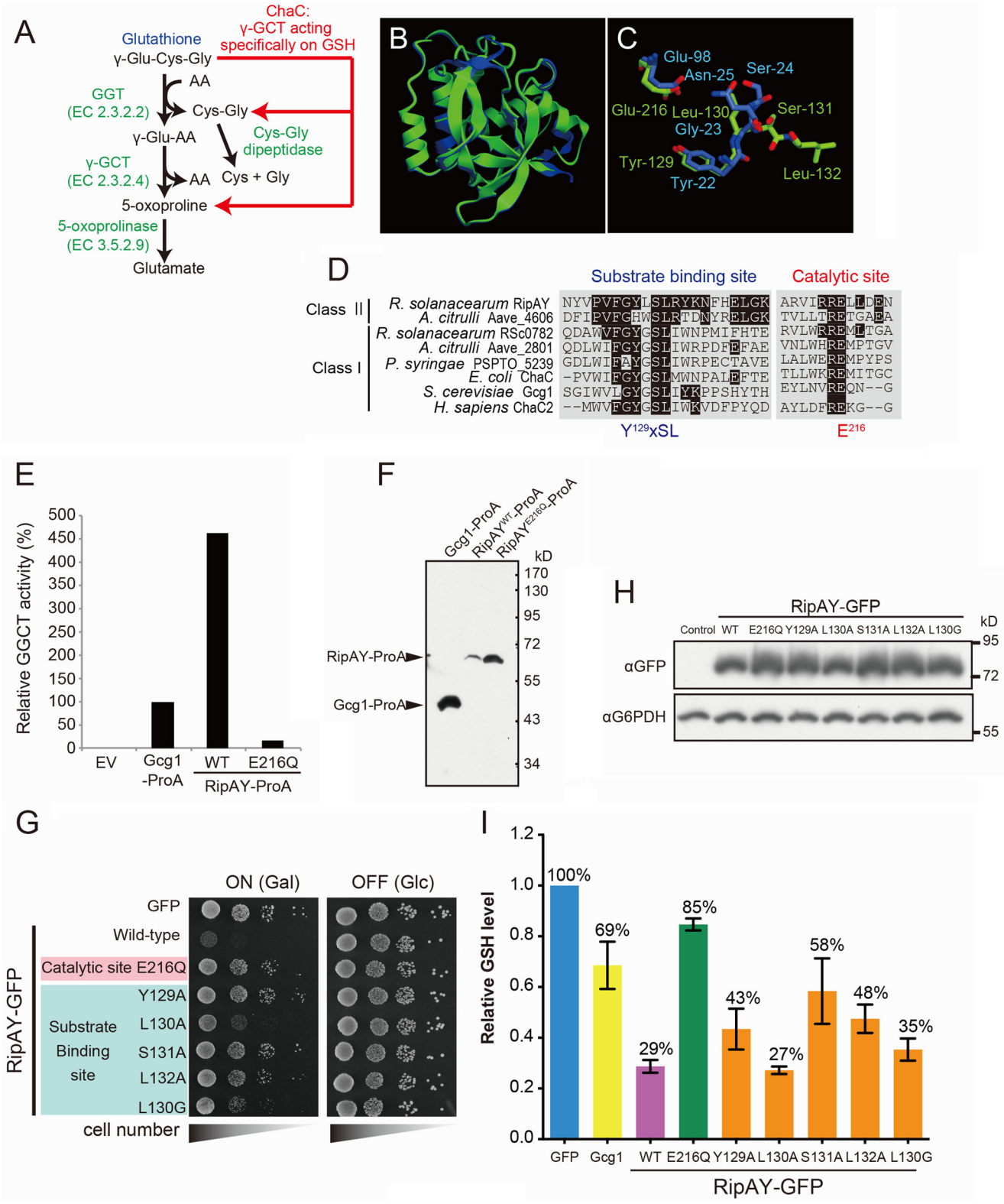

we performed an inoculation test of *R. solanacearum* WT and *ripAY*-deficient (Δ*ripAY*) cells into eggplant leaf mesophyll tissues. We observed typical necrotic lesions in the area inoculated with both *R. solanacearum* WT and Δ*ripAY* cells at 2 days postinoculation but not in the area inoculated with a T3SS mutant, Δ*hrcU*, and control mock (Fig. 4*A*), indicating that RipAY is dispensable for virulence of *R. solanacearum* on eggplant.

We next examined glutathione levels in eggplant leaves inoculated with *R. solanacearum*. Lysates were extracted from the area inoculated with *R. solanacearum* WT, Δ*ripAY*, and Δ*hrcU* cells and control mock at 1 day postinoculation, and then the total glutathione level of these lysates was analyzed (Fig. 4*B*). We observed a modest decrease of glutathione in Δ*hrcU*-inoculated eggplant leaves (decreased to 79% relative to the control), indicating that a pathogen-associated molecular pattern-triggered immunity response may affect the host glutathione homeostasis. Strikingly, eggplant leaves inoculated with *R. solanacearum* WT showed a significant decrease in glutathione (decreased to 40% relative to the control), whereas eggplant leaves inoculated with Δ*ripAY* did not show any significant decrease (Fig. 4*B*), implying that RipAY functions as a GGCT in host plant cells during *R. solanacearum* infection.

RipAY GGCT Activity Is Triggered by a Eukaryotic Factor—To perform a detailed enzyme kinetic analysis of GGCT activity of RipAY toward glutathione, recombinant RipAY and Gcg1 proteins were purified from *E. coli* using His_6 tag and nickel-nitrilotriacetic acid affinity chromatography (Fig. 5*A*), and their GGCT activity was determined by a Dug1-coupled assay (18). As shown in Fig. 5*B*, the recombinant Gcg1 protein showed significant GGCT activity toward glutathione, as described previously (18). However, we failed to detect GGCT activity of recombinant RipAY, although we could detect robust GGCT activity in RipAY expressed in yeast (Fig. 2*C*). Based on these results, we hypothesized that RipAY might acquire its GGCT activity from an activator harbored in yeast cells but not in *E. coli* cells. To test this hypothesis, the beads bound with recombinant Protein A-tagged $RipAY^{WT}$ or $RipAY^{E216Q}$ proteins expressed in *E. coli* were preincubated with a yeast extract, and then GGCT activity of the beads was measured. As shown in Fig. 5*C*, yeast extract could stimulate the GGCT activity of $RipAY^{WT}$ but not that of catalytically inactive $RipAY^{E216Q}$ in a dose-dependent manner, showing that yeast extract contains the activator(s) for RipAY. We did not observe any size changes in RipAY proteins after treatment with yeast extract (Fig. 5*D*), indicating that activation of RipAY is not dependent on cleavage or modification of the protein. Furthermore, not only a yeast extract, but also other eukaryotic cell extracts, including those of human cultured cells (HeLa) and two plants, *A. thaliana* and eggplant (*S. melongena*), but not that of *R. solanacearum*, could stimulate GGCT activity of a bacterially expressed RipAY-His_6 protein (Fig. 5*E*). These data demonstrated that RipAY acquires its GGCT activity by a eukaryote-specific factor.

Purification and Identification of the Activator for RipAY from Yeast Extract—Heat treatment (95 °C for 5 min) or extensive dialysis of the yeast extract did not eliminate the activation of RipAY, but proteinase K treatment completely eliminated it, suggesting that the activator must be heat-stable and proteinaceous (data not shown). To identify the activator of RipAY from a yeast extract, a biochemical approach was employed. Proteins extracted from yeast cells were sequentially fractionated by anion exchange, hydrophobic interaction, and gel filtration chromatography (Fig. 6*A*). Fractions were assayed for their ability to stimulate GGCT activity of RipAY. Those GGCT stimulation activities from the final purification step were analyzed by Tricine SDS-PAGE (Fig. 6*B*). A single 11-kDa protein was correlated with activity (fractions 37–41). Mass spectrometry identified this protein as Trx1 and Trx2 proteins, isoenzymes of yeast cytoplasmic thioredoxin (Trx) (Fig. 6*C*).

Yeast Thioredoxins Can Stimulate GGCT Activity of RipAY Both in Vivo and in Vitro—The yeast proteome contains three Trx isoenzymes: two cytoplasmic isoenzymes (Trx1 and Trx2) and one mitochondrial isoenzyme (Trx3). Because RipAY is expressed in the cytoplasm in yeast cells (Fig. 1*E*), we expected that the growth inhibition effect caused by RipAY must be eliminated by simultaneous deletion of its candidate activators, Trx1 and Trx2. RipAY and Gcg1 proteins were expressed under the control of the doxycycline-repressible *Tet-off* promoter (33) in yeast WT, *trx3*Δ single-, *trx1*/*2*Δ double-, and *trx1*/*2*/*3*Δ triple-mutant cells, and the growth of yeast was scored by a spot assay (Fig. 7*A*). Interestingly, we observed that overexpression of Gcg1 also causes growth inhibition in both *trx1*/*2*Δ and *trx1*/*2*/*3*Δ mutants (Fig. 7*A*, *bottom*), suggesting that a subtle

FIGURE 2. **Expression of RipAY in yeast causes growth inhibition by depletion of intracellular glutathione through its conserved ChaC domain.** *A*, the GSH catabolism by a classical γ-glutamyl transpeptidase- and GGCT-dependent pathway and a novel ChaC family-dependent pathway. *GGT*, γ-glutamyl transpeptidase. *B*, the RipAY protein was modeled using the Phyre2 server. The homology model obtained was superimposed on the crystal structure of GGCT (C7orf24, Protein Data Bank codes 2PN7 and 2RBH) using the graphics program CueMol. Shown is superimposition of homology-modeled RipAY structure (*green*) on GGCT structure (*blue*). *C*, putative active site residues of RipAY (Y^{129}LSL and Glu^{216}; *green*) were superimposed on corresponding active site residues of GGCT (Y^{22}GSN and Glu^{98}; *blue*). *D*, multiple alignment of amino acid sequences in the regions of putative substrate binding and catalytic sites of the class I and II ChaC proteins. The conserved amino acids, Y^{129}*X*SL and Glu^{216}, are the putative substrate binding site and catalytic glutamate residue for GGCT, respectively. *E*, Protein A-tagged Gcg1, RipAY WT, and active site mutant, E216Q, were expressed in a glutathione-degrading enzyme-deficient strain (*dug3*Δ *ecm38*Δ *gcg1*Δ triple mutant) of yeast cells and immunopurified with IgG-beads. The GGCT activity of the beads immobilized with Gcg1, $RipAY^{WT}$, or $RipAY^{E216Q}$ proteins was measured by a Dug1-coupled method as described under "Experimental Procedures." *EV*, empty vector. *F*, the proteins extracted from the beads shown in *E* were resolved on SDS-PAGE followed by immunoblotting using a rabbit IgG. *G*, mutations in putative substrate binding and catalytic sites of RipAY restore the yeast growth inhibition caused by expression of RipAY. Yeast cells carrying empty vector or *GAL1* expression vector of WT or the indicated mutant proteins of RipAY were spotted on SD (−Ura) and SGal (−Ura) plates and cultured for 2 days and 3 days, respectively. *H*, yeast cells carrying *GAL1* expression plasmid of GFP-tagged WT or the indicated mutant proteins of RipAY were grown in SD (−Ura) liquid medium to mid-log phase and then shifted to SGal (−Ura) liquid medium to induce the protein expression, further cultured for 12 h, and analyzed by immunoblotting with anti-GFP antibody. *I*, mutations in putative substrate binding and catalytic sites of RipAY restore the reduction of intracellular GSH level in yeast caused by expression of RipAY. The total GSH levels of the cell lysates from yeast cells expressing the indicated proteins were measured as described under "Experimental Procedures." Values represent the mean ± S.E. (*error bars*) ($n \geq 3$).

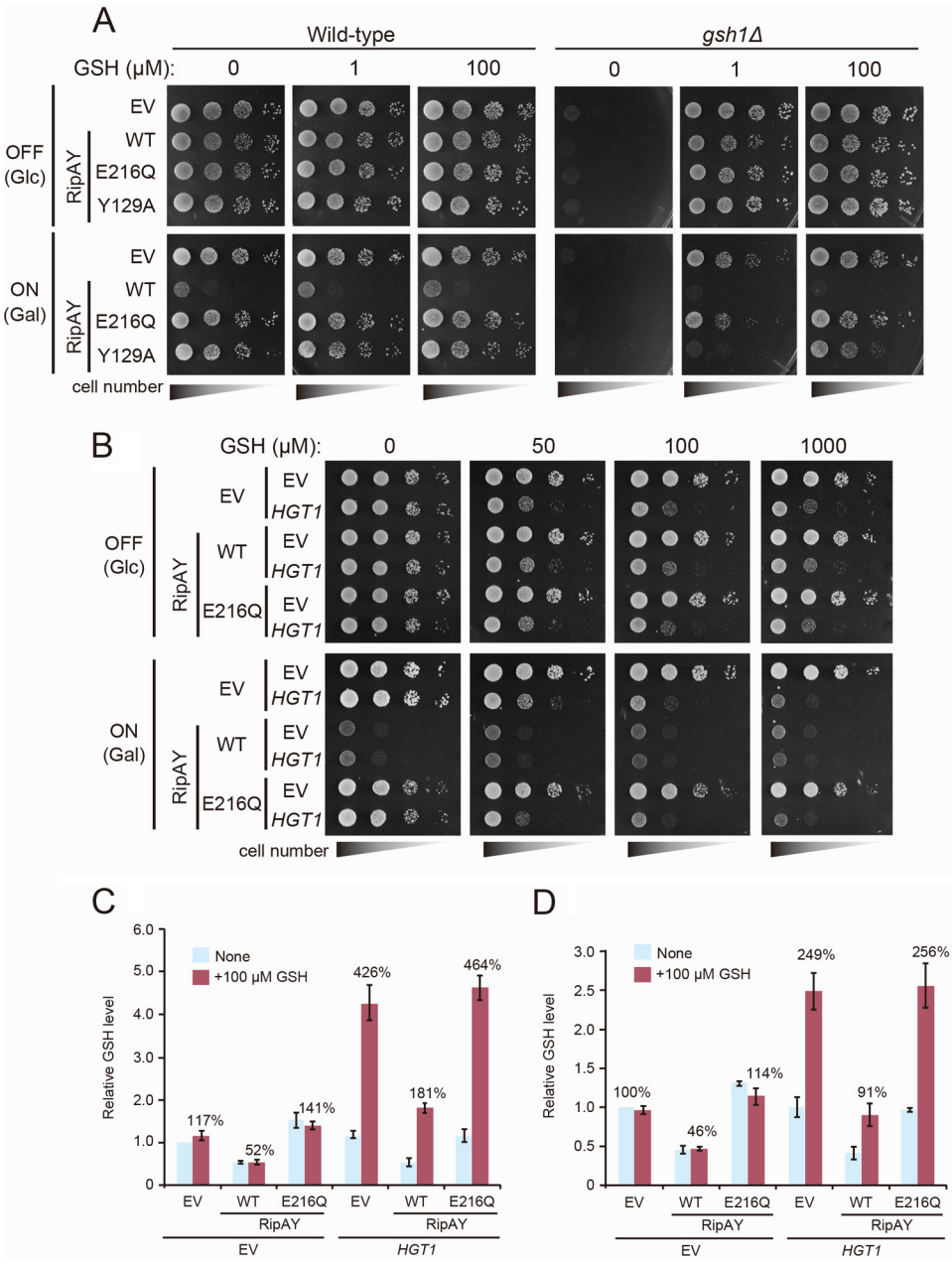

FIGURE 3. **Increased uptake of GSH does not rescue the growth inhibition effect caused by expression of RipAY.** *A*, yeast wild-type and *gsh1*Δ/*gsh1*Δ homozygote cells carrying the indicated plasmids were spotted on SD (−Ura) (*OFF*) or SGal (−Leu, −Ura) (*ON*) plates supplemented with the indicated concentration of GSH. *EV*, empty vector. Cells were incubated at 26 °C for 2 days for SD (−Leu, −Ura) or 3 days for SGal (−Leu, −Ura). *B*, yeast cells carrying the indicated plasmids were spotted on SD (−Leu, −Ura) (RipAY expression: *OFF*) or SGal (−Leu, −Ura) (RipAY expression: *ON*) plates supplemented with the indicated concentration of GSH. Cells were incubated at 26 °C for 2 days for SD (−Leu, −Ura) or 3 days for SGal (−Leu, −Ura). RipAY or *HGT1* were expressed under the control of a galactose-inducible *GAL1* promoter or a strong constitutive *TEF1* promoter, respectively. *C*, yeast cells carrying the indicated plasmids growing exponentially in SD (−Leu, −Ura) liquid medium were transferred to SGal (−Leu, −Ura) liquid medium and cultured at 26 °C for 19 h, and then GSH (100 μM) was supplemented at 30 min before termination of the culture. *D*, yeast cells carrying indicated plasmids growing exponentially in SD (−Leu, −Ura) liquid medium were transferred to SGal (−Leu, −Ura) liquid medium supplemented with or without 100 μM GSH and cultured at 26 °C for 19 h. The total GSH levels of the cell lysates from yeast cells expressing indicated proteins were measured. Values represent the mean ± S.E. (*error bars*) ($n = 4$ for *C* and $n = 3$ for *D*).

decrease of glutathione in Trx-deficient cells causes growth inhibition because the Trx system shares some redundant functions in cellular redox homeostasis with the glutathione system (34). Contrary to our expectation, we still observed the growth-inhibitory effect by expression of RipAY in *trx1*/2Δ mutant cells (Fig. 7*A*, *third bottom panel*). However, an additional deletion of *TRX3* from *trx1*/2Δ mutant (*trx1*/2/3Δ) clearly restored the growth inhibition (Fig. 7*A*, *bottom right panel*). Consistent with these results, lysate from *trx1*/2/3Δ cells almost completely lost the activation activity of RipAY, whereas lysate from *trx1*/2Δ cells still retained weak but significant activation activity (Fig. 7*B*). In addition, the lysate from *trx3*Δ cells could activate GGCT activity of RipAY, and also *trx3*Δ cells expressing RipAY exhibited growth inhibition. These data indicate that the major activators for RipAY in yeast cells must be Trx1 and Trx2. Finally, we demonstrated that a bacterially expressed Trx1-His_6

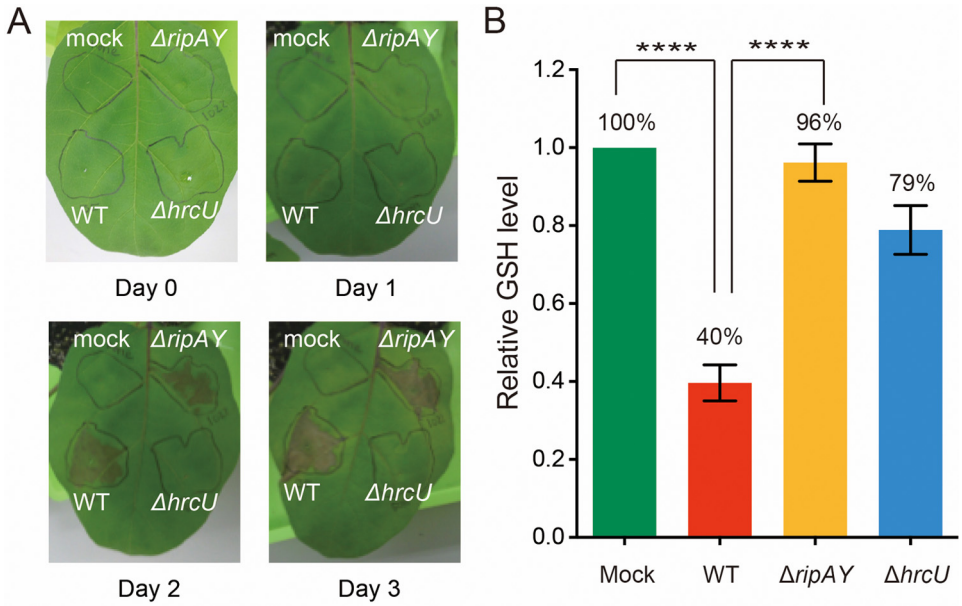

FIGURE 4. **The GSH level of eggplant leaves inoculated with *R. solanacearum* wild-type, RipAY-deficient, and T3SS-deficient strains.** *A*, necrotic lesions on eggplant leaf 3 days postinoculation with *R. solanacearum* WT strain (*WT*), RipAY-deficient strain (Δ*ripAY*), or T3SS-deficient strain (Δ*hrcU*). *Mock*, inoculation of buffer without bacteria as a control. *B*, the GSH level of total lysate extracted from eggplant leaves inoculated with the indicated *R. solanacearum* strains at 1 day postinoculation was measured as described under "Experimental Procedures." Values represent the mean ± S.E. (*error bars*) ($n \geq 7$). ****, $p < 0.0001$, one-way analysis of variance post hoc test (Turkey's multiple comparison test).

protein could stimulate GGCT activity of RipAY *in vitro* (Fig. 7*C*). Taken together, these results demonstrated that yeast Trxs could stimulate GGCT activity of RipAY both *in vivo* and *in vitro*.

Plant Trxs Bind to and Activate RipAY in an Isoform-specific Manner—Next, we investigated whether plant Trxs could also activate RipAY. Because *Arabidopsis* extract could activate RipAY *in vitro* (Fig. 5*E*) and Trxs from *Arabidopsis* are relatively well characterized, we employed the *Arabidopsis* Trxs for this purpose. The *Arabidopsis* genome encodes 19 Trxs belonging to six major groups: f, m, h, o, x, and y (35). Whereas most of these Trxs are located in chloroplasts and mitochondria, the h-type Trxs, which consist of eight isoenzymes, are generally thought to be located in the cytoplasm. Among these h-type Trxs in *Arabidopsis*, *At*Trx-h2 has the highest similarity to yeast Trxs (Fig. 8*F*). Furthermore, *At*Trx-h3 is the most highly constitutively expressed cytoplasmic Trx, and *At*Trx-h5 is substantially up-regulated upon infection with *Pseudomonas syringae* (36). We therefore chose these three *Arabidopsis* Trxs as candidate activators for RipAY. We first tested whether RipAY directly interacted with Trxs using yeast two-hybrid analysis. As shown in Fig. 8*A*, we could detect the interaction of RipAY with all eukaryotic Trxs tested but not with *R. solanacearum* Trx, *Rs*TrxA, under both low and medium stringency conditions (−Trp/−Leu/−His and −Trp/−Leu/−His/+3-amino-1,2,4-triazole, respectively). However, we could detect the interaction of RipAY with only *At*Trx-h5 under high stringency conditions (−Trp/−Leu/−His/−Ade), indicating that RipAY binds *At*Trx-h5 with higher affinity than the other eukaryotic Trxs in yeast two-hybrid analysis. Trxs catalyze disulfide reduction through a redox-active site, WC*X*PC (34). We also examined whether redox-active disulfide residues of *At*Trx-h5 are required for the binding to RipAY. The redox-inactive mutant *At*Trx-h5^{CS}, in which active site cysteine residues at positions 39 and 42 were substituted by serine, showed decreased binding and activation activity relative to the WT but still bound to RipAY and exhibited significant activation activity (Fig. 8, *A* and *E*). Moreover, the RipAY^{CS} mutant, in which the sole cysteine residue at position 333 was substituted by serine, also bound to both the WT and the redox-inactive mutant of *At*Trx-h5. Furthermore, heterologous expression of the RipAY^{CS} mutant caused growth inhibition of yeast (Fig. 8*B*), and recombinant RipAY^{CS} mutant protein expressed in *E. coli* exhibited Trx-dependent activation *in vitro*, which was similar to that of RipAY^{WT} (Fig. 8, *C* and *D*). Taken together, these data indicate that the eukaryotic Trxs bind to RipAY without intermolecular disulfide binding-dependent covalent interaction.

We next tested whether the plant Trxs stimulated GGCT activity of RipAY *in vitro*. The GGCT activity of RipAY toward glutathione was measured in the presence of various concentrations of each recombinant Trx isoenzyme. As shown in Fig. 8*E*, *At*Trx-h5 could most effectively stimulate GGCT activity of RipAY (>10-fold compared with *At*Trx-h2: 0.790 ± 0.073 μM/s at 5 μM *At*Trx-h5 *versus* 0.066 ± 0.009 μM/s at 5 μM *At*Trx-h2). Interestingly, the RipAY activation activity of Trxs was correlated with the RipAY binding ability of Trxs (order of RipAY activation activity: *At*Trx-h5 > *At*Trx-h3 > *Sc*Trx1 ≫ *At*Trx-h2 ≥ *At*Trx-h5^{CS}). The addition of *Rs*TrxA to RipAY failed to stimulate GGCT activity, consistent with its inability to bind RipAY. Taken together, these data showed that plant Trxs bind to RipAY and stimulate its GGCT activity in an isoform-specific manner.

Because heterologous expression of RipAY, but not the other ChaC proteins, caused growth inhibition of yeast (Fig. 1*C*) and a marked decrease of intracellular glutathione in yeast cells (Fig. 2*F*), we speculated that the catalytic efficiency of RipAY might

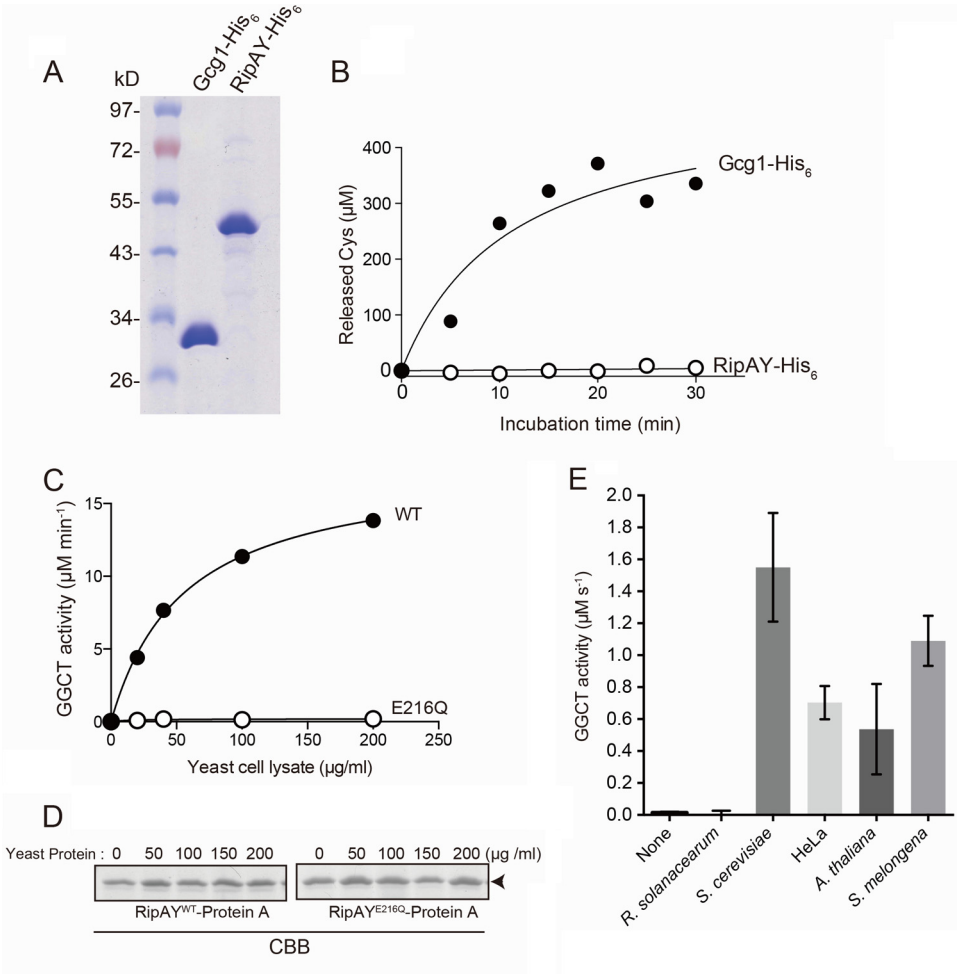

FIGURE 5. **RipAY exhibits GGCT activity in the presence of eukaryotic factor(s).** *A*, purification of recombinant Gcg1 and RipAY proteins. Recombinant His_6-tagged Gcg1 and RipAY were expressed in *E. coli* and purified using nickel-nitrilotriacetic acid affinity chromatography. Purified proteins were analyzed on SDS-PAGE with Coomassie Blue staining. *B*, measurement of GGCT activity of recombinant Gcg1 and RipAY purified from *E. coli*. 0.1 μg of Gcg1 and 1 μg of RipAY were incubated with 5 mM glutathione, the reactions were terminated at the indicated time points, the released Cys-Gly dipeptides were digested with Cys-Gly dipeptidase Dug1, and then the released Cys was measured by acidic ninhydrin. *C*, effect of concentration of the yeast protein extract on activation of GGCT activity of RipAY. The beads bound with $RipAY^{WT}$ or $RipAY^{E216Q}$ proteins expressed in *E. coli* were preincubated with different concentrations of native yeast protein extracted from a glutathione-degrading enzyme-deficient strain (*dug3*Δ *ecm38*Δ *gcg1*Δ triple mutant) for 2 h at 4 °C and washed with the same buffer three times, and then GGCT activity of the beads was measured by the Dug1-coupled method. *D*, the Protein A-tagged $RipAY^{WT}$ and $RipAY^{E216Q}$ proteins extracted from the beads shown in *C* were resolved on SDS-PAGE and visualized by Coomassie Brilliant Blue (*CBB*) staining. *E*, the GGCT activity of bacterially expressed RipAY-His_6 protein incubated with 10 μg of protein of the cell lysates from *R. solanacearum*, *S. cerevisiae*, human cultured cell HeLa, *A. thaliana*, or eggplant *S. melongena* cells was measured by a Dug1-coupled method. Values represent the mean ± S.E. (*error bars*) ($n \geq 3$).

be much higher than that of the class I ChaC proteins. To confirm this speculation, we performed kinetic analysis of RipAY and Gcg1 toward glutathione and compared their kinetic parameters. Both RipAY, which was activated by 8 μM *At*Trx-h5, and Gcg1 showed Michaelis-Menten kinetics toward glutathione (Fig. 9, *A* and *B*). We observed some inhibition at high substrate (glutathione) concentrations. The kinetic parameters revealed similar K_m values for both Gcg1 (1.23 ± 0.17 mM) and RipAY (2.11 ± 0.17 mM), although the k_{cat} values were markedly different; the k_{cat} value of RipAY was 160-fold higher than that of Gcg1 (52.8 ± 9.58 s^{-1} for RipAY *versus* 0.33 ± 0.02 s^{-1} for Gcg1) (Table 4). Furthermore, the specificity constant, k_{cat}/K_m value of RipAY is 94-fold higher than that of Gcg1 (25.2 ± 1.22 s^{-1}/mM for RipAY *versus* 0.27 ± 0.03 s^{-1}/mM for Gcg1). Collectively, we clearly demonstrated that the catalytic efficiency of RipAY is much higher than that of the class I ChaC protein.

Discussion

The T3SS effector proteins exhibit various molecular activities that generally allow bacteria to escape from host immune systems and break down barriers for pathogen growth and dissemination. Uncovering the molecular functions of T3SS effector proteins is therefore one of the most important subjects for a mechanistic understanding of pathogenesis (4). In this study, we revealed that a ChaC domain-containing effector protein, RipAY, from the plant pathogenic bacterium *R. solanacearum* modulates the abundance of host intracellular glutathione by acting as a eukaryotic thioredoxin-dependent GGCT.

Expression of RipAY Causes Growth Inhibition in Yeast—We initially identified RipAY as one of the *R. solanacearum* effectors whose expression causes growth inhibition in yeast (Fig. 1*C*). Subsequent analysis revealed that this growth inhibition effect might be caused by a decrease in glutathione, which is

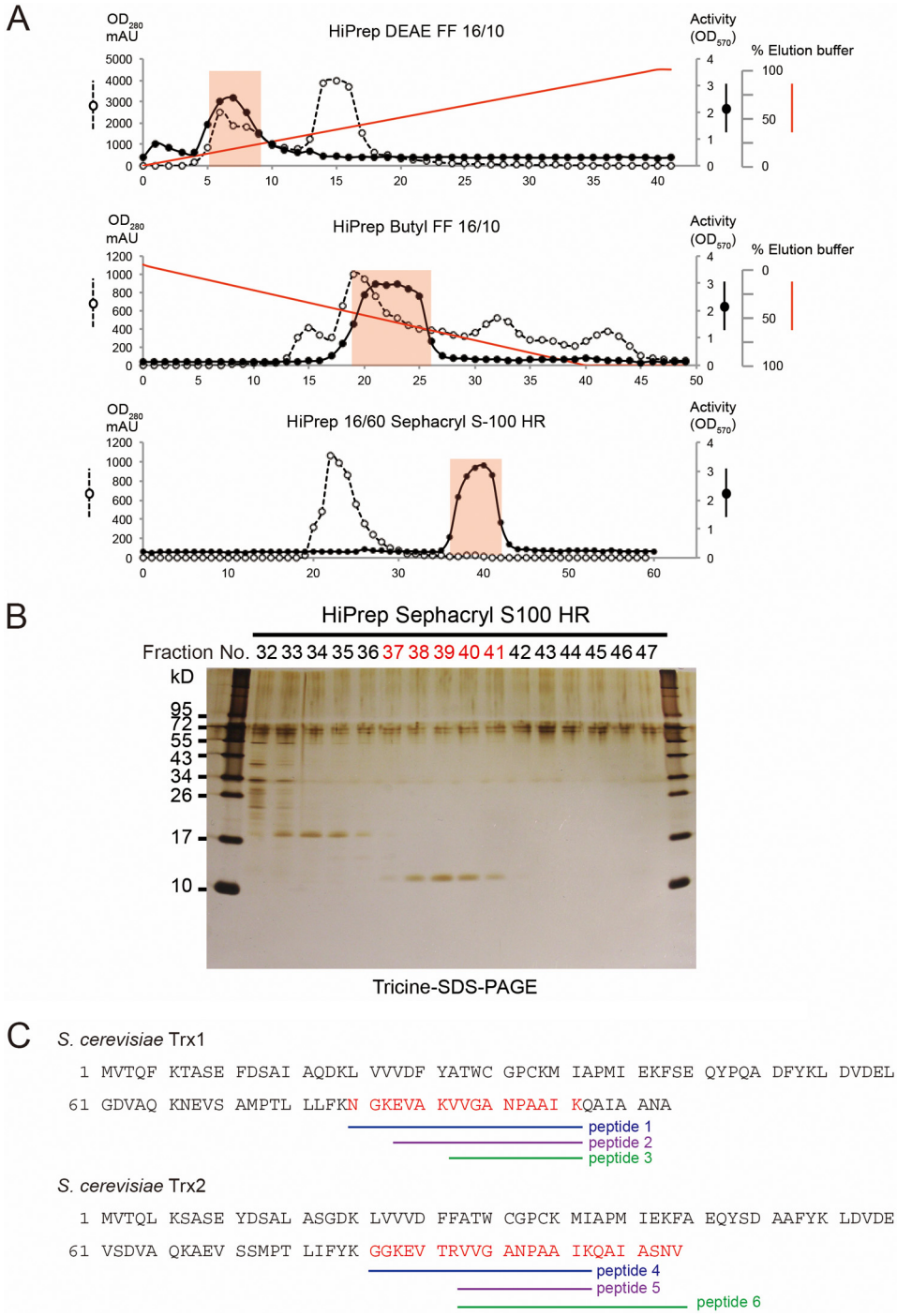

FIGURE 6. **Identification of thioredoxin as a eukaryotic activator for GGCT activity of RipAY.** *A*, biochemical purification of the eukaryotic activator of RipAY from yeast protein extracts by HiPrep DEAE FF 16/10 ion exchange, HiPrep Butyl FF 16/10 hydrophobic interaction, and HiPrep 16/60 Sephacryl S-100 HR gel filtration chromatography. *B*, gel filtration fractions surrounding activity were loaded onto a Tricine SDS-polyacrylamide gel, visualized by silver staining. *C*, gel bands of fractions 37–41 stained with Coomassie Brilliant Blue were collected and in-gel digested, and following LC-MS/MS analysis, yeast thioredoxin Trx1 and Trx2 proteins were identified as the activator. Amino acid sequences of *S. cerevisiae* Trx1 and Trx2 and their corresponding tryptic peptides identified by LC-MS/MS analysis are shown.

dependent on a ChaC domain in RipAY (Fig. 2, *E* and *F*). Kumar *et al.* (18) reported that expression of human CHAC1 in yeast mutant cells with limited glutathione availability leads to apoptosis through depletion of intracellular glutathione, and this effect is rescued by the addition of exogenous glutathione. Unexpectedly, we found that the addition of exogenous glutathione failed to rescue the growth inhibition caused by expression of RipAY (Fig. 3*A*). Furthermore, overexpression of Hgt1 in RipAY-expressing cells could not restore the growth inhibition on media containing glutathione, although the intracellular glutathione level was almost restored in this condition (Fig. 3, *B* and *C*). Importantly, because mutation in the putative catalytic site completely restored the growth inhibition, this effect is dependent on GGCT activity of RipAY (Fig. 3*B*). These data

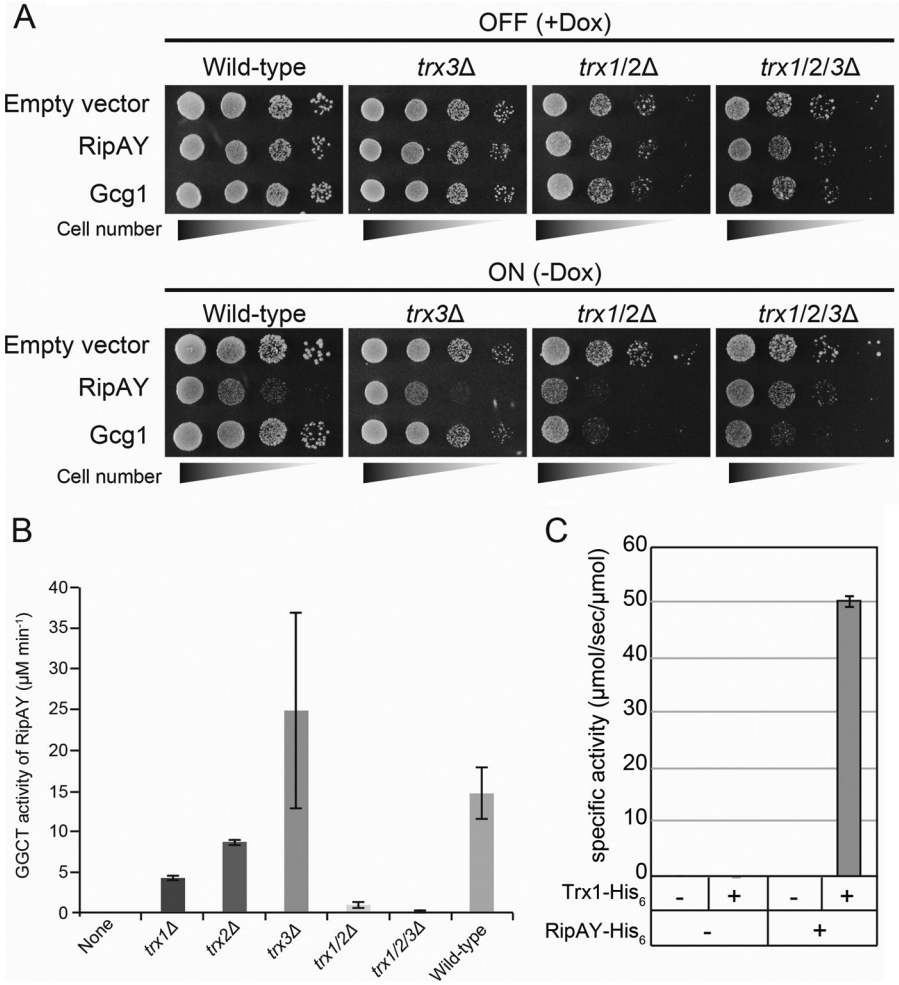

FIGURE 7. **Yeast thioredoxins can activate a GGCT activity of RipAY both *in vivo* and *in vitro*.** *A*, *S. cerevisiae* WT, *trx3*Δ single mutant, *trx1/2*Δ double mutant, and *trx1/2/3*Δ triple mutant cells carrying plasmid expressing RipAY or Gcg1 under the control of the *Tet-off* promoter were grown in noninducing (+*Dox*) or inducing (−*Dox*) conditions. Yeast cells transformed with corresponding empty vector were used as a control. The cells were grown at 26 °C for 3 days for SD (−Ura, +Dox) and 4 days for SD (−Ura, −Dox). *B*, the GGCT activity of bacterially expressed RipAY-His_6 protein incubated with 10 μg of protein of the cell lysates from the indicated *S. cerevisiae* thioredoxin mutant cells was measured by the Dug1-coupled method. Values represent the mean ± S.E. (*error bars*) ($n \geq 3$). *C*, bacterially expressed *S. cerevisiae* Trx1-His_6 protein can activate the GGCT activity of bacterially expressed RipAY-His_6 protein.

clearly indicate that yeast growth inhibition must be a consequence of RipAY-dependent degradation of another yet unidentified γ-glutamyl compound(s) rather than glutathione. Recently, Chi *et al.* (37) reported that mouse CHAC1/Botch, which promotes embryonic neurogenesis through inhibition of Notch signaling, deglycinates the γ-glutamyl-glycine at position 1,669 of Notch to prevent the S1 furin-like cleavage of Notch. Further analysis will be required to understand the molecular mechanisms underlying the yeast growth inhibition observed in the expression of RipAY.

RipAY Is a Novel Type of Effector That Targets Host Glutathione—To our knowledge, RipAY is the first T3SS effector targeting host intracellular glutathione. Glutathione has been repeatedly reported to play a crucial role in plant immune responses during biotic stresses (20). For instance, the *Arabidopsis pad2-1* mutant, which was originally identified as a phytoalexin camalexin-deficient mutant, was shown to be mutated in γ-glutamylcysteine synthetase (Gsh1), a critical enzyme that catalyzes the first committed step in glutathione synthesis (38). Mutant *pad2-1* plants fail to accumulate significant levels of glutathione and are rendered highly susceptible to biotrophic pathogens and insects (19). Oppositely, an enhanced level of glutathione by expression of *GSH1* in tobacco (*Nicotiana tabacum*) confers biotic stress tolerance, probably thorough the disease resistance-priming gene, *NPR1*-dependent salicylic acid-mediated pathway (39). Furthermore, *Arabidopsis* knock-out mutants for one of two glutathione reductase genes, *GR1*, which show a constitutive increase in oxidized glutathione, accumulate less plant defense hormone, salicylic acid, than the WT and show increased sensitivity to virulent *P. syringae* (40). We show that inoculation of *R. solanacearum* WT into eggplant leaves causes a significant decrease of glutathione, and mutation of RipAY in *R. solanacearum* restores this glutathione decrease (Fig. 3*B*). Taken together, these results indicate that RipAY affects the host immune response by decreasing host intracellular glutathione. However, despite the importance of RipAY for host glutathione homeostasis, an *R. solanacearum* mutant lacking RipAY was not attenuated for virulence toward eggplant (Fig. 4*A*), arguing for the existence of additional effector proteins that interfere with a host disease-resistant signaling pathway. Indeed, a systematic effector knock-out approach for *R. solanacearum* failed to identify mutants with reduced

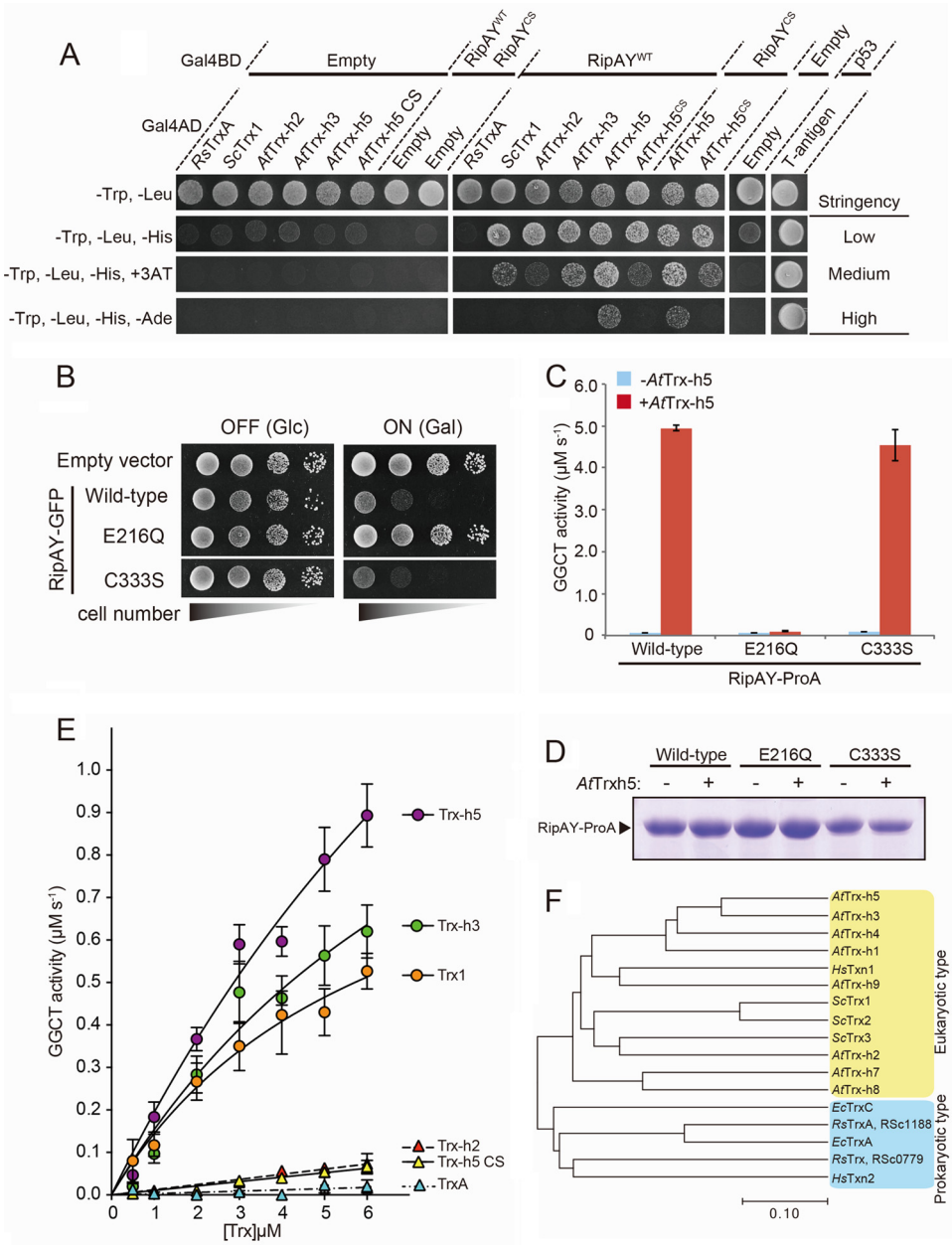

FIGURE 8. **Plant thioredoxins can bind to RipAY and activate GGCT activity of RipAY in an isoform-specific manner.** *A*, yeast two-hybrid assay for interaction between RipAY and various thioredoxins on the plate with different stringency conditions. RipAY WT (RipAY^{WT}) and a mutant form of RipAY (RipAY^{CS}), in which the sole cysteine residue at position 333 was substituted by serine, were used as bait. *R. solanacearum* TrxA (*Rs*TrxA), *S. cerevisiae* Trx1 (*Sc*Trx1), *A. thaliana* Trx-h2, -h3, and -h5 (*At*Trx-h2, *At*Trx-h3, and *At*Trx-h5), and a mutant form of Trx-h5 (*At*Trx-h5^{CS}), in which active site cysteine residues at position 39 and 42 were substituted by serine, were used as prey. *B*, yeast cells carrying empty vector or *GAL1* expression vector of WT, active site mutant E216Q, or C333S mutant of RipAY were spotted on SD (−Ura) and SGal (−Ura) plates and cultured for 2 days and 3 days, respectively. *C*, GGCT activity of the beads bound with Protein A-tagged RipAY^{WT}, RipAY^{E216Q}, or RipAY^{C333S} proteins expressed in *E. coli* incubated with 1.6 μM *At*Trx-h5-His$_6$ protein was measured by the Dug1-coupled method. Values represent the mean ± S.E. (*error bars*) ($n = 3$). *D*, Protein A-tagged RipAY^{WT}, RipAY^{E216Q}, and RipAY^{C333S} proteins extracted from the beads shown in *C* were resolved on SDS-PAGE and visualized by Coomassie Brilliant Blue staining. *E*, effect of thioredoxin isoforms on activation of GGCT activity of RipAY. The GGCT activity of RipAY incubated with various concentrations of thioredoxin isoforms was measured by the Dug1-coupled method. Values represent the mean ± S.E. ($n \geq 3$). *F*, phylogenetic analysis of thioredoxin isoforms from various organisms. The organisms, locus tag/gene name, and Genbank^{TM} accession numbers (in parentheses) are as follows: *R. solanacearum*, RSc1188/*Rs*TrxA (AL646052.1) and RSc0779/*Rs*Trx (AL646052.1); *E. coli*, *Ec*TrxA (M26133.1) and *Ec*TrxC (U8594.1); *H. sapiens*, *Hs*Txn1 (JQ313905.1) and *Hs*Txn2 (DQ891579.2); *S. cerevisiae*, YLR043C/*Sc*Trx1 (NM_001181930.1), YGR209C/*Sc*Trx2 (NM_001181338.3), and YCR083C/*Sc*Trx3 (NM_001178789.1); *A. thaliana*, At3g51030/*At*Trx-h1 (NM_114963.4), At5g39950/*At*Trx-h2 (AY113052.1), At5g42980/*At*Trx-h3 (AY065098.1), At1g19730/*At*Trx-h4 (BT004710.1), At1g45145/*At*Trx-h5 (AY040028.1), At1g59730/*At*Trx-h7 (BT0031540.1), At1g69880/*At*Trx-h8 (BT003670.1), and At3g08710/*At*Trx-h9 (BT0011728.1).

pathogenicity on two host plants, indicating a functional overlap among effectors (41).

Regulation of the Abundance of Host Intracellular Glutathione by RipAY—Given that most bacterial pathogens translocate only trace amounts of their effector proteins into host cell cytoplasm (42), it seemed that RipAY must be a GGCT with extremely high catalytic efficiency to decrease host intracellular glutathione during *R. solanacearum* infection. In fact, our enzyme kinetic analysis revealed that the k_{cat} value of Trx-h5-activated RipAY was much higher than that of a *S. cerevisiae*

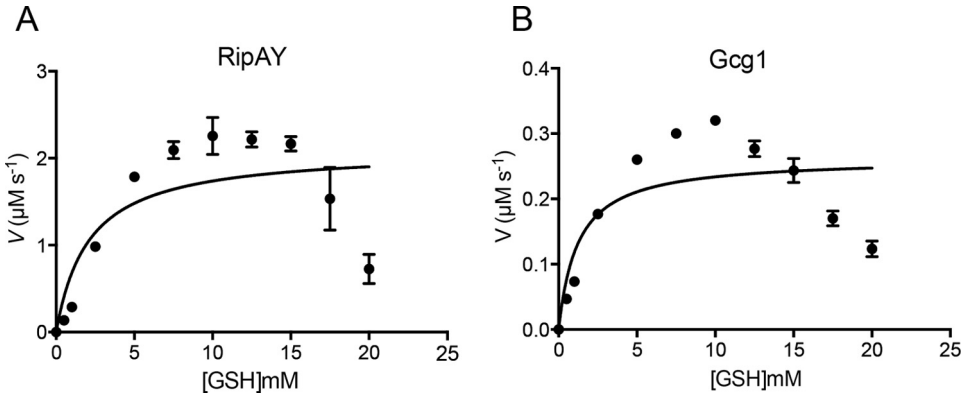

FIGURE 9. **Enzyme kinetic analysis of activated RipAY and Gcg1.** Shown is a Michaelis-Menten plot of Trx-h5-activated RipAY (*A*) and Gcg1 (*B*) toward glutathione. Gcg1 (0.8 μM) or RipAY (0.04 μM) in the presence of Trx-h5 (8 μM) was used for determination of kinetic parameters. Different concentrations of glutathione were used ranging from 0.5 to 20 mM. Dug1-coupled assay was used for the study as described under "Experimental Procedures." Data of three independent experiments were analyzed by non-linear regression using GraphPad prism version 6.0. *Error bars*, S.E.

TABLE 4
Kinetic parameters of *S. cerevisiae* Gcg1 and *At*Trx-h5-activated RipAY

Enzyme	K_m	k_{cat}	k_{cat}/K_m	Comparison of k_{cat}/K_m value *versus* RipAY		
				Gcg1	*At*GGCT2;2[a]	*At*GGCT2;3[a]
	mM	s^{-1}	$s^{-1}\ mM^{-1}$	*-fold*		
Gcg1	1.23 ± 0.17	0.33 ± 0.02	0.27 ± 0.03			
RipAY[b]	2.11 ± 0.17	52.8 ± 9.58	25.2 ± 1.22	94.0	66.7	1,081

[a] Data from Kumar *et al.* (29).
[b] RipAY was activated by 8 μM *At*Trx-h5.

class I ChaC protein, Gcg1 (160-fold), although both activated RipAY and Gcg1 show a similar K_m value (Table 4). Recently, Kumar *et al.* (29) reported a detailed enzyme kinetic analysis of *Arabidopsis* ChaC orthologues, *At*GGCT2;2 and *At*GGCT2;3. Based on their data, we estimated that the k_{cat}/K_m value of RipAY is 66.7- and 1,081-fold higher than that of *At*GGCT2;2 and *At*GGCT2;3, respectively (Table 4). This extremely high catalytic efficiency of thioredoxin-activated RipAY compared with the intrinsic class I ChaC proteins is logical, because probably very limited amounts of the bacterial effector are efficiently translocated inside the plant host cells. Injection of a very active RipAY could allow depletion of the host intracellular glutathione during *R. solanacearum* infection.

Activation of RipAY by Eukaryotic Thioredoxins—A truly unexpected finding was that for RipAY to exhibit GGCT activity, it has to be bound and activated by host plant cytoplasmic thioredoxins in an isoform-specific manner (Fig. 8*E*). Recent findings provide remarkable examples for the emerging concept of spatiotemporal regulation of pathogen effectors by coupling the catalytic activity to the arrival into a host cell's cytoplasm (42–46). The mechanism of activation coupled with T3SS-dependent delivery ensures that eukaryotic cells are specifically and potently targeted and that the bacterium is protected from the toxic effects of its own enzymatic activity (46). Interestingly, the GGCT activity of RipAY is stimulated by thioredoxins, which are relatively well conserved within both prokaryotes and eukaryotes, and the *R. solanacearum* genome also contains five thioredoxin or thioredoxin-like proteins. Our data suggest that eukaryotic but not prokaryotic thioredoxin(s) can specifically bind to RipAY and stimulate GGCT activity of RipAY (Fig. 8, *A* and *E*). Phylogenic tree analysis revealed that eukaryotic-type thioredoxins are clearly divided from prokaryotic-type thioredoxins (Fig. 8*F*). As one might expect, our results raise two interesting questions regarding how RipAY recognizes eukaryotic thioredoxins in an isoform-specific manner and how thioredoxins stimulate the GGCT activity of RipAY. Further studies will be required for a better understanding of the mechanisms underlying thioredoxin recognition and the enzyme activation of RipAY at the molecular level.

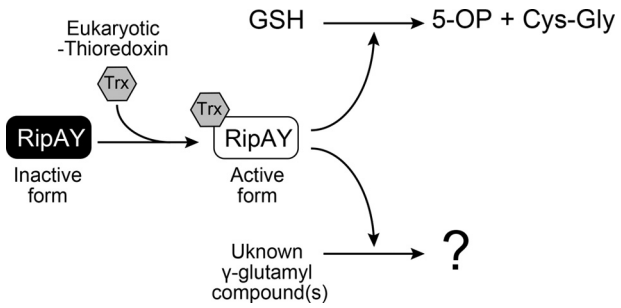

FIGURE 10. **A model depicting how the RipAY T3SS effector is activated by host eukaryotic thioredoxins to trigger GGCT activity.** RipAY was injected into a host plant cell as an inactive form, and then its GGCT activity was stimulated by host eukaryotic thioredoxins, such as Trx-h5, to degrade glutathione and other unknown γ-glutamyl compound(s). *5-OP*, 5-oxoproline.

A Working Model for the Role of RipAY during R. solanacearum Infection—Pathogen infection induces the expression of several thioredoxins in *Arabidopsis* (36, 47). In particular, Trx-h5 plays an important role in plant defense because it was shown that Trx-h5 facilitates the reduction of NPR1 disulfides to catalyze the oligomer-to-monomer switch, which in turn promotes the activation of salicylic acid-dependent plant defense (36). Intriguingly, we found that Trx-h5 could most efficiently stimulate the GGCT activity of RipAY *in vitro* (Fig. 8*E*). Based on this observation, we speculate that

RipAY is injected into the host plant cell via the T3SS apparatus as an inactive form and then converted to an active form by host eukaryotic thioredoxins, in particular Trx-h5, during *R. solanacearum* infection and then degrades glutathione and other unknown γ-glutamyl compounds, which together might prevent the activation of the host disease response (Fig. 10). Further analysis will be required to understand the role of RipAY during *R. solanacearum* infection at the molecular level.

Author Contributions—S. F. and M. T. designed the experiments; S. F., K. O., T. Kitagawa, C. P., T. Kawazoe, and M. T. performed the experiments; K. N., Y. K., S. G., and M. V. contributed new reagents/analytic tools; S. F., N. T., and M. T. analyzed data; and M. T. wrote the paper. All authors reviewed the results and approved the final version of the manuscript.

Acknowledgments—We thank Tomoe Nakagawa and Jun-ichi Hasegawa for contributions to the initial experiments. We also thank Dr. Yasuomi Tada and Nodoka Oka (Nagoya University) for valuable advice and for supplying A. thaliana cDNA clones. We are grateful to Drs. Goro Takata and Akihide Yoshihara for technical assistance in operating the ÄKTA Explorer system. We acknowledge the technical expertise of the DNA core facility of the Gene Research Center, Kagawa University. We express our deep appreciation to Prof. Anand Bachhawat for generously providing pTEF-416-HGT1 plasmid and for valuable discussion of the data and critical reading of the manuscript.

References

1. Dean, P. (2011) Functional domains and motifs of bacterial type III effector proteins and their roles in infection. *FEMS Microbiol. Rev.* **35,** 1100–1125
2. Bhavsar, A. P., Guttman, J. A., and Finlay, B. B. (2007) Manipulation of host-cell pathways by bacterial pathogens. *Nature* **449,** 827–834
3. Galán, J. E. (2009) Common themes in the design and function of bacterial effectors. *Cell Host Microbe.* **5,** 571–579
4. Deslandes, L., and Rivas, S. (2012) Catch me if you can: bacterial effectors and plant targets. *Trends Plant Sci.* **17,** 644–655
5. Siggers, K. A., and Lesser, C. F. (2008) The Yeast *Saccharomyces cerevisiae*: a versatile model system for the identification and characterization of bacterial virulence proteins. *Cell Host Microbe.* **4,** 8–15
6. Valdivia, R. H. (2004) Modeling the function of bacterial virulence factors in *Saccharomyces cerevisiae*. *Eukaryot. cell* **3,** 827–834
7. Lesser, C. F., and Miller, S. I. (2001) Expression of microbial virulence proteins in *Saccharomyces cerevisiae* models mammalian infection. *EMBO J.* **20,** 1840–1849
8. Salanoubat, M., Genin, S., Artiguenave, F., Gouzy, J., Mangenot, S., Arlat, M., Billault, A., Brottier, P., Camus, J. C., Cattolico, L., Chandler, M., Choisne, N., Claudel-Renard, C., Cunnac, S., Demange, N., *et al.* (2002) Genome sequence of the plant pathogen *Ralstonia solanacearum*. *Nature* **415,** 497–502
9. Genin, S. (2010) Molecular traits controlling host range and adaptation to plants in *Ralstonia solanacearum*. *New Phytol.* **187,** 920–928
10. Coll, N. S., and Valls, M. (2013) Current knowledge on the *Ralstonia solanacearum* type III secretion system. *Microb. Biotechnol.* **6,** 614–620
11. Genin, S., and Denny, T. P. (2012) Pathogenomics of the *Ralstonia solanacearum* species complex. *Annu. Rev. Phytopathol.* **50,** 67–89
12. Deslandes, L., and Genin, S. (2014) Opening the *Ralstonia solanacearum* type III effector tool box: insights into host cell subversion mechanisms. *Curr. Opin. Plant Biol.* **20,** 110–117
13. Peeters, N., Carrère, S., Anisimova, M., Plener, L., Cazalé, A. C., and Genin, S. (2013) Repertoire, unified nomenclature and evolution of the Type III effector gene set in the *Ralstonia solanacearum* species complex. *BMC Genomics* **14,** 859
14. Angot, A., Peeters, N., Lechner, E., Vailleau, F., Baud, C., Gentzbittel, L., Sartorel, E., Genschik, P., Boucher, C., and Genin, S. (2006) *Ralstonia solanacearum* requires F-box-like domain-containing type III effectors to promote disease on several host plants. *Proc. Natl. Acad. Sci. U.S.A.* **103,** 14620–14625
15. Poueymiro, M., Cazalé, A. C., François, J. M., Parrou, J. L., Peeters, N., and Genin, S. (2014) A *Ralstonia solanacearum* type III effector directs the production of the plant signal metabolite trehalose-6-phosphate. *mBio* 10.1128/mBio.02065-14
16. Le Roux, C., Huet, G., Jauneau, A., Camborde, L., Trémousaygue, D., Kraut, A., Zhou, B., Levaillant, M., Adachi, H., Yoshioka, H., Raffaele, S., Berthomé, R., Couté, Y., Parker, J. E., and Deslandes, L. (2015) A receptor pair with an integrated decoy converts pathogen disabling of transcription factors to immunity. *Cell* **161,** 1074–1088
17. Mukaihara, T., Tamura, N., and Iwabuchi, M. (2010) Genome-wide identification of a large repertoire of *Ralstonia solanacearum* type III effector proteins by a new functional screen. *Mol. Plant Microbe. Interact.* **23,** 251–262
18. Kumar, A., Tikoo, S., Maity, S., Sengupta, S., Sengupta, S., Kaur, A., and Bachhawat, A. K. (2012) Mammalian proapoptotic factor ChaC1 and its homologues function as γ-glutamyl cyclotransferases acting specifically on glutathione. *EMBO Rep.* **13,** 1095–1101
19. Spoel, S. H., and Loake, G. J. (2011) Redox-based protein modifications: the missing link in plant immune signalling. *Curr. Opin. Plant Biol.* **14,** 358–364
20. Dubreuil-Maurizi, C., and Poinssot, B. (2012) Role of glutathione in plant signaling under biotic stress. *Plant Signal. Behav.* **7,** 210–212
21. Ito, H., Fukuda, Y., Murata, K., and Kimura, A. (1983) Transformation of intact yeast cells treated with alkali cations. *J. Bacteriol.* **153,** 163–168
22. Imai, Y., Matsushima, Y., Sugimura, T., and Terada, M. (1991) A simple and rapid method for generating a deletion by PCR. *Nucleic Acids Res.* **19,** 2785
23. Tamura, K., Stecher, G., Peterson, D., Filipski, A., and Kumar, S. (2013) MEGA6: Molecular Evolutionary Genetics Analysis version 6.0. *Mol. Biol. Evol.* **30,** 2725–2729
24. Rahman, I., Kode, A., and Biswas, S. K. (2006) Assay for quantitative determination of glutathione and glutathione disulfide levels using enzymatic recycling method. *Nat. Protoc.* **1,** 3159–3165
25. Kanda, A., Yasukohchi, M., Ohnishi, K., Kiba, A., Okuno, T., and Hikichi, Y. (2003) Ectopic expression of *Ralstonia solanacearum* effector protein PopA early in invasion results in loss of virulence. *Mol. Plant Microbe. Interact.* **16,** 447–455
26. Kuramitsu, Y., Miyamoto, H., Tanaka, T., Zhang, X., Fujimoto, M., Ueda, K., Tanaka, T., Hamano, K., and Nakamura, K. (2009) Proteomic differential display analysis identified upregulated astrocytic phosphoprotein PEA-15 in human malignant pleural mesothelioma cell lines. *Proteomics* **9,** 5078–5089
27. Poueymiro, M., and Genin, S. (2009) Secreted proteins from *Ralstonia solanacearum*: a hundred tricks to kill a plant. *Curr. Opin. Microbiol.* **12,** 44–52
28. Ivey, D. M., Guffanti, A. A., Zemsky, J., Pinner, E., Karpel, R., Padan, E., Schuldiner, S., and Krulwich, T. A. (1993) Cloning and characterization of a putative Ca^{2+}/H^{+} antiporter gene from *Escherichia coli* upon functional complementation of Na^{+}/H^{+} antiporter-deficient strains by the overexpressed gene. *J. Biol. Chem.* **268,** 11296–11303
29. Kumar, S., Kaur, A., Chattopadhyay, B., and Bachhawat, A. K. (2015) Defining the cytosolic pathway of glutathione degradation in *Arabidopsis thaliana*: role of the ChaC/GCG family of γ-glutamyl cyclotransferases as glutathione-degrading enzymes and AtLAP1 as the Cys-Gly peptidase. *Biochem. J.* **468,** 73–85
30. Oakley, A. J., Yamada, T., Liu, D., Coggan, M., Clark, A. G., and Board, P. G. (2008) The identification and structural characterization of C7orf24 as γ-glutamyl cyclotransferase: an essential enzyme in the γ-glutamyl cycle. *J. Biol. Chem.* **283,** 22031–22042
31. Bourbouloux, A., Shahi, P., Chakladar, A., Delrot, S., and Bachhawat, A. K. (2000) Hgt1p, a high affinity glutathione transporter from the yeast *Saccharomyces cerevisiae*. *J. Biol. Chem.* **275,** 13259–13265

32. Kumar, C., Igbaria, A., D'Autreaux, B., Planson, A. G., Junot, C., Godat, E., Bachhawat, A. K., Delaunay-Moisan, A., and Toledano, M. B. (2011) Glutathione revisited: a vital function in iron metabolism and ancillary role in thiol-redox control. *EMBO J.* **30,** 2044–2056
33. Tabuchi, M., Kawai, Y., Nishie-Fujita, M., Akada, R., Izumi, T., Yanatori, I., Miyashita, N., Ouchi, K., and Kishi, F. (2009) Development of a novel functional high-throughput screening system for pathogen effectors in the yeast *Saccharomyces cerevisiae*. *Biosci. Biotechnol. Biochem.* **73,** 2261–2267
34. Meyer, Y., Buchanan, B. B., Vignols, F., and Reichheld, J. P. (2009) Thioredoxins and glutaredoxins: unifying elements in redox biology. *Annu. Rev. Genet.* **43,** 335–367
35. Gelhaye, E., Rouhier, N., Navrot, N., and Jacquot, J. P. (2005) The plant thioredoxin system. *Cell Mol. Life Sci.* **62,** 24–35
36. Tada, Y., Spoel, S. H., Pajerowska-Mukhtar, K., Mou, Z., Song, J., Wang, C., Zuo, J., and Dong, X. (2008) Plant immunity requires conformational changes [corrected] of NPR1 via *S*-nitrosylation and thioredoxins. *Science* **321,** 952–956
37. Chi, Z., Byrne, S. T., Dolinko, A., Harraz, M. M., Kim, M. S., Umanah, G., Zhong, J., Chen, R., Zhang, J., Xu, J., Chen, L., Pandey, A., Dawson, T. M., and Dawson, V. L. (2014) Botch is a γ-glutamyl cyclotransferase that deglycinates and antagonizes Notch. *Cell Rep.* **7,** 681–688
38. Parisy, V., Poinssot, B., Owsianowski, L., Buchala, A., Glazebrook, J., and Mauch, F. (2007) Identification of PAD2 as a γ-glutamylcysteine synthetase highlights the importance of glutathione in disease resistance of *Arabidopsis*. *Plant J.* **49,** 159–172
39. Ghanta, S., Bhattacharyya, D., Sinha, R., Banerjee, A., and Chattopadhyay, S. (2011) *Nicotiana tabacum* overexpressing γ-ECS exhibits biotic stress tolerance likely through NPR1-dependent salicylic acid-mediated pathway. *Planta* **233,** 895–910
40. Mhamdi, A., Hager, J., Chaouch, S., Queval, G., Han, Y., Taconnat, L., Saindrenan, P., Gouia, H., Issakidis-Bourguet, E., Renou, J. P., and Noctor, G. (2010) *Arabidopsis* GLUTATHIONE REDUCTASE1 plays a crucial role in leaf responses to intracellular hydrogen peroxide and in ensuring appropriate gene expression through both salicylic acid and jasmonic acid signaling pathways. *Plant Physiol.* **153,** 1144–1160
41. Cunnac, S., Occhialini, A., Barberis, P., Boucher, C., and Genin, S. (2004) Inventory and functional analysis of the large Hrp regulon in *Ralstonia solanacearum*: identification of novel effector proteins translocated to plant host cells through the type III secretion system. *Mol. Microbiol.* **53,** 115–128
42. Gaspar, A. H., and Machner, M. P. (2014) VipD is a Rab5-activated phospholipase A1 that protects *Legionella pneumophila* from endosomal fusion. *Proc. Natl. Acad. Sci. U.S.A.* **111,** 4560–4565
43. Fu, H., Coburn, J., and Collier, R. J. (1993) The eukaryotic host factor that activates exoenzyme S of *Pseudomonas aeruginosa* is a member of the 14-3-3 protein family. *Proc. Natl. Acad. Sci. U.S.A.* **90,** 2320–2324
44. Christen, M., Coye, L. H., Hontz, J. S., LaRock, D. L., Pfuetzner, R. A., Megha, and Miller, S. I. (2009) Activation of a bacterial virulence protein by the GTPase RhoA. *Sci. Signal.* **2,** ra71
45. Coaker, G., Falick, A., and Staskawicz, B. (2005) Activation of a phytopathogenic bacterial effector protein by a eukaryotic cyclophilin. *Science* **308,** 548–550
46. Anderson, D. M., Schmalzer, K. M., Sato, H., Casey, M., Terhune, S. S., Haas, A. L., Feix, J. B., and Frank, D. W. (2011) Ubiquitin and ubiquitin-modified proteins activate the *Pseudomonas aeruginosa* T3SS cytotoxin, ExoU. *Mol. Microbiol.* **82,** 1454–1467
47. Laloi, C., Mestres-Ortega, D., Marco, Y., Meyer, Y., and Reichheld, J. P. (2004) The *Arabidopsis* cytosolic thioredoxin h5 gene induction by oxidative stress and its W-box-mediated response to pathogen elicitor. *Plant Physiol.* **134,** 1006–1016